The modeling of turbulent reactive flows based on multiple mapping conditioning

A. Y. Klimenko[a)] and S. B. Pope
Sibley School of Mechanical and Aerospace Engineering, Cornell University, Ithaca, New York 14853

A new modeling approach—multiple mapping conditioning (MMC)—is introduced to treat mixing and reaction in turbulent flows. The model combines the advantages of the probability density function and the conditional moment closure methods and is based on a certain generalization of the mapping closure concept. An equivalent stochastic formulation of the MMC model is given. The validity of the closuring hypothesis of the model is demonstrated by a comparison with direct numerical simulation results for the three-stream mixing problem. © *2003 American Institute of Physics.* [DOI: 10.1063/1.1575754]

I. INTRODUCTION

Turbulent combustion models have been developing for the last 30 years and, at present, they represent powerful tools for analyzing combustion processes in turbulent flows.[1–3] Probability density function (PDF) models[4,5] provide the most detailed information about the stochastic characteristics of all species involved in a combustion process, and this allows for the most accurate evaluation of the reaction rates. However, for the realistic chemical processes involving hundreds of species, the complete direct evaluation of the joint PDFs of all reactive species does not seem feasible at present (this would require solving equations in the composition space whose dimension is expressed by a three-digit number). The computationally efficient PDF methods are expected to reduce the effective number of dimensions to an acceptable two-digit number using certain automatic reduction techniques.[6,7]

The ideas developed in the present work are based on the presumption that, practically, it is not necessary to allow all species to fluctuate in all possible ways. First, fluctuations of concentrations are restricted by the conservation of elements and other conservation principles. Second, fast reactions force some of the concentrations to be asymptotically close to their partial equilibrium states. Third, some of the turbulent fluctuations do not have a significant effect on combustion and can be neglected. We use the word "major" to characterize fluctuations or composition manifolds (i.e., curved surfaces in the composition space of a dimension smaller than the dimension of the whole space), which are taken into account by the model; and the word "minor" characterizes fluctuations that are neglected or composition manifolds that are not attainable. The same minor/major notations can be used to characterize species: the term "major species" emphasizes that fluctuations of this particular set of species are not restricted, while the term "minor species" refers to species that are allowed to fluctuate only jointly with the major species. (Note that, for a given major manifold, the selection of major species is not unique and we do not restrict our consideration to a specific choice of the major species.) Practically, this means that the concentrations of the minor species are conditioned on the concentrations of the major species. Thus, in the present work, we also have to deal with the models analyzing the evolution of the conditional expectations.

The model that deals with the conditional expectations of the reactive components is the conditional moment closure (CMC).[8] Although this model can be formulated for multiple conditions, the practical realizations of the model are mostly limited to the values conditioned on a single variable (normally the mixture fraction). The model provides a relatively computationally inexpensive alternative to the evaluation of the joint PDF of all reactive scalars, but it often lacks the ability to take into account some of the significant fluctuations of the reactive species (the fluctuations with respect to the conditional means) in order to determine the reaction rates accurately. One possible solution is to introduce a conditional variance equation and determine the reaction rates with the use of a presumed conditional PDF based on the calculated conditional variance.[8,9] Another way of improving the accuracy of the conditional models is to take into account more of the turbulent fluctuations by increasing the number of conditioning variables. This means that instead of using the mixture fraction as the only conditioning variable, we use several conditioning variables (which can be represented by the concentrations of the major species). Another link of equations for conditional expectations and PDF models is discussed in Refs. 10, 11 for velocity-type conditioning.

In spite of the relative transparency of these ideas, their practical implementation is not easy. The difficulties are not in formulating the conditional equations with multiple conditioning variables—these equations are well known.[8] (The possibility of using the scalar dissipation as an additional conditioning variable is explored by Cha *et al.*[12]) The mixture fraction based CMC needs the specification of the one-

variable PDF of the mixture fraction, but the conditional closures with multiple conditions would require the specification of the multidimensional joint PDF for the major species. While the shapes of the mixture fraction PDF are well known and can be presumed, determining the joint PDF of the major (reactive) species needs more extensive PDF modeling.

The present work represents a logical combination of the PDF method, which is used to find the joint PDFs in the major manifold, and conditional methods, which are used to determine the evolution of the dependent species. This work goes far beyond mechanistic combining of two different methods into one model. It appears that the model suggested in the present work does not discriminate between the major and minor species, but treats them in the same way (i.e., the PDF/CMC interpretations of the model are valid for any reasonable choice of major and minor species).

As in any PDF method, the PDF part of the present model needs a closure. An additional difficulty is induced by the fact that CMC needs the specification, not only of the PDF of the major species, but also of their conditional dissipation, which has to be consistent with the joint PDF. This problem has been solved in the present work by generalizing the concept of mapping closure (MC).[13,14] For the statistically homogeneous case, the major idea in the mapping closure is to consider the mapping between n_s Gaussian reference fields and the n_s species concentration fields. This mapping (which is not unique) is constructed to yield the known one-point joint PDF of the species. Then, statistics of the species fields (in particular, the conditional dissipation) are determined from the joint PDF and the mapping. Thus, a closure is achieved, which takes the form of an evolution equation for the mapping. For a single species ($n_s=1$), the mapping closure has been fully explored[13–17] and particle implementations have been developed.[14,18,19] The application of the mapping closure for multiple species ($n_s>1$) has also been considered.[14,20,21] However, a computationally tractable implementation that respects the mapping closure and scalar linearity and independence principles has yet to be developed.

In contrast to previous works, we introduce a new version of MC that (a) from its origin is formulated for inhomogeneous flows, (b) deals with multidimensional spaces without any need of artificial ordering of the variables, and (c) allows for non-Gaussian distributions for the reference variable (although the specific form of the present closure is, as the original MC, implemented with Gaussian reference variables). Considering its link with MC, and the multidimensional nature of the model we refer to the new method as the model with *multiple mapping conditioning* (MMC). The MMC model is introduced in Sec. II, where its properties are analyzed. The MMC model matches well properties of turbulent mixing such as localness,[22,23] boundedness, independence of scalars[24] and Gaussianity of the PDFs in appropriate limits. Although we refer to MMC as a model, the MMC approach is more akin to a certain framework that can be used to formulate various specific models.

A significant part of the paper (Secs. III and IV) is devoted to an equivalent stochastic (i.e., Monte Carlo) formulation and implementation of the MMC model. Although the dimension of the major composition manifold is smaller than the total number of species, this dimension is, generally, not expected to be small. For multidimensional spaces, stochastic formulations are expected to be more computationally efficient than deterministic formulations.[4] The most difficult part of the stochastic formulation is, as usual, the evaluation of the mixing step, which requires the calculation of certain conditional averages. In the present work we suggest the method of diffusing clouds, which has some similarities with the method of smoothed particle hydrodynamics,[25] but the diffusing clouds are allowed to expand in time. For this method the numerical diffusion which is associated with the evaluation of the conditional averages matches the intensity of the diffusion required by the MMC model.

Another problem considered in Sec. IV is related to the formulation of the initial conditions. Assuming that appropriate initial conditions are specified for all species, the MMC model also has to be provided with an initial mapping of the concentrations into the reference Gaussian space. For multiple dimensions this mapping is not unique. Without the claiming of finding an ultimate solution for this problem, we suggest a procedure—"mapping by preferential directions" (MPD)—which is based on some additional physical considerations and a certain ordering of the variables or their linear combinations. Although the scalars in MPD are not independent (as they are in MMC), we believe that this method corresponds well to the physics of the problem for a large class of practical cases.

In the last section, we consider the problem of three-stream mixing that has been simulated numerically by Juneja and Pope[26] (JP in further references). This problem should probably serve as a benchmark problem for all multivariable joint PDF closures. It is shown that, for the MMC model, this problem has an analytical solution that is compared with numerical calculations using the diffusing clouds method. The analytical MMC results match well the DNS results of JP while the stochastic simulations are in good agreement with the analytical formulas.

II. DETERMINISTIC FORMULATION OF THE MMC MODEL

A. Major and minor species

We consider a set of n_s chemically active species, with mass fractions $Y_I(\mathbf{x},t)$, $(I=1,2,\ldots,n_s)$ that satisfy the transport equation

$$\frac{\partial \rho Y_I}{\partial t} + \nabla\cdot(\mathbf{v}\rho Y_I) - \nabla\cdot(D\nabla Y_I) = \rho\Omega_I, \tag{1}$$

where $\mathbf{v}=\mathbf{v}(\mathbf{x},t)$ is the fluid velocity, D is the diffusion coefficient (which is assumed to be the same for all species), ρ is the density, and Ω_I is the rate of creation of species I due to chemical reactions. Both ρ and Ω_I are assumed to be known functions of the mass fractions: $\Omega_I=\Omega_I(\mathbf{Y})$, $\rho=\rho(\mathbf{Y})$. [For simplicity of exposition, we confine attention to this set of species, although in practice an energy variable (e.g., enthalpy) must also be considered. However, since the

enthalpy equation has the same form of (1), it is trivial to extend the present treatment to the general case.]

A fundamental assumption in the model is that, at $(\mathbf{x},t)$, the compositions $\mathbf{Y}(\mathbf{x},t)$ that occur in different realizations of the flow are restricted to an n_r-dimensional manifold in the n_s-dimensional composition space $(n_r < n_s)$. This manifold is denoted by $\mathbf{Z}(\boldsymbol{\xi},\mathbf{x},t)$, where $\boldsymbol{\xi}=\{\xi_1,\xi_2,\ldots,\xi_{n_r}\}$ are reference variables that parametrize the manifold, and $\mathbf{Z}$ has n_s components $\{Z_1,Z_2,\ldots,Z_{n_s}\}$. The assumption that $\mathbf{Y}(\mathbf{x},t)$ is restricted to this manifold is then written as

$$\mathbf{Y}(\mathbf{x},t) = \mathbf{Z}(\boldsymbol{\xi}^*,\mathbf{x},t), \tag{2}$$

where $\boldsymbol{\xi}^* \equiv \{\xi_1^*,\xi_2^*,\ldots,\xi_{n_r}^*\}$ is a random point in the reference $\boldsymbol{\xi}$ space. Note that $\mathbf{Z}(\boldsymbol{\xi},\mathbf{x},t)$ is a deterministic function, and the randomness of $\mathbf{Y}(\mathbf{x},t)$ is reflected in the randomness of $\boldsymbol{\xi}^*$.

An important special case to consider is that in which there is a set of n_r "major species" such that there is a one-to-one mapping between the manifold and the mass fractions of these major species. We denote by $\mathbf{Y}_{\{i\}}$ the mass fractions of the major species, and by $\mathbf{Y}_{\{\alpha\}}$ the mass fractions of the remaining $n_s - n_r$ "minor" species. In this case, knowledge of the major species $\mathbf{Y}_{\{i\}}$ determines a unique point on the manifold, and hence the mass fractions $\mathbf{Y}_{\{\alpha\}}$ of the minor species. Thus, the minor species are (by assumption) determined by the major species; and so there are no fluctuations in the minor species about their means conditioned on the major species. These conditional means are denoted by

$$Q_\alpha(\mathbf{Y}_{\{i\}},\mathbf{x},t) = \langle Y_\alpha(\mathbf{x},t) | \mathbf{Y}_{\{i\}}(\mathbf{x},t) = \mathbf{y}_{\{i\}} \rangle. \tag{3}$$

Locally on the manifold (i.e., in the neighborhood of a general point $\boldsymbol{\xi}^p$), it is always possible to find a set of n_r species such that their mass fractions have a one-to-one mapping with points on the manifold. But, if the manifold has folds, a set of "major" species (for which, globally, there is a one-to-one mapping) may not exist. In the model presented below, there is no assumption about the existence of major species, and indeed all species are treated equally. However, some of the properties of the model are deduced, assuming the existence of major species. Furthermore, some concepts are more easily understood, and the model is more obviously related to CMC, when major species exist—as is assumed in this and the next section.

Before proceeding, we clarify the notation used for subsets of species. Bracketed subscripts are used to specify the span of a vector when clarification of the dimensionality of the vector is needed. For example, Y_I (upper case Roman suffix) is a value indexed by a running index I, while $\mathbf{Y}_{\{I\}}$ represents the whole set $\{Y_1,Y_2,\ldots\}$, as determined by the span of the dummy index I. If the dummy index is not specified, then the vector involves all relevant components: $\mathbf{Y} = \{Y_1,Y_2,\ldots,Y_{n_s}\}$. A major species is denoted by Y_i (lower case Roman suffix), and the complete set of n_r major species by $\mathbf{Y}_{\{i\}}$. Similarly, a minor species is denoted by Y_α (lower case Greek suffix), and the complete set of $n_s - n_r$ minor

species by $\mathbf{Y}_{\{\alpha\}}$. The sample-space variables are denoted by $\mathbf{y}$ for all species; by $\mathbf{y}_{\{I\}}$ for some subset; by $\mathbf{y}_{\{i\}}$ for major species; and by $\mathbf{y}_{\{\alpha\}}$ for minor species.

B. The PDF and CMC equations

An accurate evaluation of the reaction rates requires the specification of the one-point joint PDF of the species mass fractions P_Y or of the Favre joint PDF $\tilde{P}_Y$. The Favre PDF of all species is denoted by $\tilde{P}_Y(\mathbf{y};\mathbf{x},t)$; of a subset by $\tilde{P}_Y(\mathbf{y}_{\{I\}};\mathbf{x},t)$; and of major species by $\tilde{P}_Y(\mathbf{y}_{\{i\}};\mathbf{x},t)$.

The transport equation for the Favre PDF, $\tilde{P}_Y$ can be derived from (1) by well-established techniques.[4,8,27] For flows with large Reynolds numbers, transport by molecular diffusion can be neglected and the PDF transport equation is given by

$$\frac{\partial \langle\rho\rangle \tilde{P}_Y}{\partial t} + \boldsymbol{\nabla}\cdot(\mathbf{u}\langle\rho\rangle\tilde{P}_Y) + \frac{\partial W_I \langle\rho\rangle\tilde{P}_Y}{\partial y_I} + \frac{\partial^2 N_{IJ}\langle\rho\rangle\tilde{P}_Y}{\partial y_I \partial y_J} = 0, \tag{4}$$

where

$$N_{IJ}(\mathbf{y}_{\{K\}};\mathbf{x},t) \equiv \langle \rho\chi_{IJ} | \mathbf{Y}_{\{K\}} = \mathbf{y}_{\{K\}} \rangle / \rho_Y, \quad \chi_{IJ} \equiv \frac{D}{\rho} \boldsymbol{\nabla} Y_I \cdot \boldsymbol{\nabla} Y_J,$$

$$\mathbf{u}(\mathbf{y}_{\{I\}};\mathbf{x},t) \equiv \langle \rho\mathbf{v} | \mathbf{Y}_{\{I\}} = \mathbf{y}_{\{I\}} \rangle / \rho_Y,$$

$$W_I(\mathbf{y}_{\{J\}};\mathbf{x},t) \equiv \langle \rho\Omega_I | \mathbf{Y}_{\{J\}} = \mathbf{y}_{\{J\}} \rangle / \rho_Y, \tag{5}$$

$$\rho_Y(\mathbf{y}_{\{I\}};\mathbf{x},t) \equiv \langle \rho | \mathbf{Y}_{\{I\}} = \mathbf{y}_{\{I\}} \rangle,$$

$$\tilde{P}_Y(\mathbf{y}_{\{I\}};\mathbf{x},t) \equiv P_Y \rho_Y / \langle\rho\rangle,$$

and the indices I, J, K run over all species or any given subset of $1,\ldots,n_s$.

If the set of species considered in the equation is complete (i.e., $\mathbf{Y}_{\{I\}} = \mathbf{Y} = \{Y_1,Y_2,\ldots,Y_{n_s}\}$), then conditional averages of the reaction rates and density are simply given by

$$W_I(\mathbf{y};\mathbf{x},t) = \Omega_I(\mathbf{y}), \quad \rho_Y(\mathbf{y};\mathbf{x},t) = \rho(\mathbf{y}). \tag{6}$$

It should be noted, however, that the joint PDF of the complete set of species is most likely singular: the PDF takes positive values only within a certain attainable manifold while remaining zero in the rest of the composition space. Thus, all PDF equations should be conventionally interpreted according their generalized sense.

As is discussed in the preceding subsection, we assume that the PDF $\tilde{P}_Y(\mathbf{y};\mathbf{x},t)$ is positive only within a certain major manifold and can be characterized by a reduced PDF of a certain smaller dimension, n_r. If a set of major species $\mathbf{Y}_{\{i\}}$, which is sufficient to characterize the major (i.e., allowed) fluctuations, is selected, then the joint PDF $\tilde{P}_Y(\mathbf{y};\mathbf{x},t)$ can be effectively replaced by the reduced PDF $\tilde{P}_Y(\mathbf{y}_{\{i\}};\mathbf{x},t)$ supplemented by the conditional expectations $Q_\alpha = Q_\alpha(\mathbf{y}_{\{i\}};\mathbf{x},t) \equiv \langle Y_\alpha | \mathbf{Y}_{\{i\}} = \mathbf{y}_{\{i\}} \rangle$. Specifically, we have

$$\tilde{P}_Y(\mathbf{y};\mathbf{x},t) = \tilde{P}_Y(\mathbf{y}_{\{i\}};\mathbf{x},t)\, \delta(\mathbf{Q}_{\{\alpha\}}(\mathbf{y}_{\{i\}};\mathbf{x},t) - \mathbf{y}_{\{\alpha\}}), \tag{7}$$

where, in general, a delta function with a vector argument denotes the product of the delta functions with the vector

components as arguments. The delta-function product in (7) is the PDF of the minor species conditional upon the major species.

Whatever the choice of the major species may be, the reduced PDF $\tilde{P}_Y(\mathbf{y}_{\{i\}};\mathbf{x},t)$ and the conditional expectations $Q_\alpha(\mathbf{y}_{\{i\}};\mathbf{x},t)$ should satisfy the equations[4,8,27]

$$\frac{\partial \langle\rho\rangle \tilde{P}_Y}{\partial t} + \boldsymbol{\nabla}\cdot(\mathbf{u}\langle\rho\rangle \tilde{P}_Y) + \frac{\partial W_i \langle\rho\rangle \tilde{P}_Y}{\partial y_i} + \frac{\partial^2 N_{ij}\langle\rho\rangle \tilde{P}_Y}{\partial y_i \partial y_j} = 0, \tag{8}$$

and

$$\frac{\partial Q_\alpha}{\partial t} + \mathbf{u}\cdot\boldsymbol{\nabla}Q_\alpha + W_i \frac{\partial Q_\alpha}{\partial y_i} - N_{ij}\frac{\partial^2 Q_\alpha}{\partial y_i \partial y_j} = W_\alpha, \tag{9}$$

where i, j, and k run over major species; α runs over minor species; $N_{ij}=N_{ij}(\mathbf{y}_{\{k\}};\mathbf{x},t)$, $\mathbf{u}=\mathbf{u}(\mathbf{y}_{\{k\}};\mathbf{x},t)$, and $\mathbf{W}=\mathbf{W}(\mathbf{y}_{\{k\}};\mathbf{x},t)$ are the scalar dissipation, velocity, and reaction rates defined in (5) and conditioned on the mass fractions of the major species. Since the major species are assumed to set a sufficient number of conditions for taking into account all major fluctuations so that the fluctuations with respect to the conditional means can be neglected, we conventionally put

$$W_I(\mathbf{y}_{\{i\}};\mathbf{x},t)\equiv\langle\Omega_I(\mathbf{Y}_{\{i\}},\mathbf{Y}_{\{\alpha\}})|\mathbf{Y}_{\{i\}}=\mathbf{y}_{\{i\}}\rangle$$
$$=\Omega_I(\mathbf{y}_{\{i\}},\mathbf{Q}_{\{\alpha\}}),$$

and

$$\rho_Y(\mathbf{y}_{\{i\}};\mathbf{x},t)\equiv\langle\rho(\mathbf{Y}_{\{i\}},\mathbf{Y}_{\{\alpha\}})|\mathbf{Y}_{\{i\}}=\mathbf{y}_{\{i\}}\rangle=\rho(\mathbf{y}_{\{i\}},\mathbf{Q}_{\{\alpha\}}),$$

in (8) and (9). Neglecting minor fluctuations also allows the neglect of the term $\tilde{P}_Y^{-1}\boldsymbol{\nabla}\cdot(\langle\mathbf{u}''(Y_\alpha)''|\mathbf{Y}_{\{i\}}=\mathbf{y}_{\{i\}}\rangle\tilde{P}_Y)$ that, otherwise, should be conventionally present in (9) (these fluctuations can be also neglected in some other cases—CMC shear flow equations,[28] for example). The double-prime superscript denotes the conditional fluctuations, for example, $(Y_\alpha)''\equiv Y_\alpha - Q_\alpha$.

It is important to observe that in (8) and (9) the only "unknowns" are the conditional mean velocity $\mathbf{u}$ and the scalar dissipation N_{ij}. Hence, if models are provided for these quantities, (8) and (9) provide a closure for species in turbulent reactive flows.

In the subsequent analysis, use is made of the conservative form of the CMC equation, which is readily obtained from (8) and (9):

$$\frac{\partial \langle\rho\rangle \tilde{P}_Y Q_\alpha}{\partial t} + \boldsymbol{\nabla}\cdot(\mathbf{u}\langle\rho\rangle \tilde{P}_Y Q_\alpha) + \frac{\partial W_i\langle\rho\rangle \tilde{P}_Y Q_\alpha}{\partial y_i}$$
$$+ \frac{\partial}{\partial y_i}\left(Q_\alpha\frac{\partial N_{ij}\langle\rho\rangle \tilde{P}_Y}{\partial y_j} - N_{ij}\langle\rho\rangle \tilde{P}_Y\frac{\partial Q_\alpha}{\partial y_j}\right) = W_\alpha\langle\rho\rangle \tilde{P}_Y. \tag{10}$$

C. The modeling equations

With the assumptions made (primarily the neglect of the conditional fluctuations of the minor species), Eqs. (8) and (9) describe the evolution of the joint PDF of the major species, $\tilde{P}_Y$, and the conditional means of the minor species

Q_α. These equations could be solved if models were available for the two unknowns—the conditional velocity $\mathbf{u}$ and the conditional dissipation N_{ij}. However, because N_{ij} appears as a negative diffusion coefficient in the PDF equation (8), the explicit modeling of N_{ij} does not lead to a stable, realizable model. Instead, we proceed indirectly (as in the mapping closure) and use the space of the reference variables to formulate the modeling equations.

The model which we can call "the model with multiple mapping conditioning" (MMC), is represented by the following equations for the n_r-dimensional manifold $\mathbf{Z}(\boldsymbol{\xi},\mathbf{x},t)$ which are to be solved in the space of the reference variables ξ_k, $k=1,2,\ldots,n_r$,

$$\frac{\partial Z_I}{\partial t} + \mathbf{U}\cdot\boldsymbol{\nabla}Z_I + A_k\frac{\partial Z_I}{\partial \xi_k} - B_{kl}\frac{\partial^2 Z_I}{\partial \xi_k \partial \xi_l} = \Omega_I(\mathbf{Z}), \tag{11}$$

where Z_I ($I=1,2,\ldots,n_s$) correspond to each of the species involved. The values of the coefficients $A_k=A_k(\boldsymbol{\xi},\mathbf{x},t)$, $B_{kl}=B_{kl}(\boldsymbol{\xi},\mathbf{x},t)$, $\mathbf{U}=\mathbf{U}(\boldsymbol{\xi},\mathbf{x},t)$ are discussed below. The solution of this equation, $Z_I=Z_I(\boldsymbol{\xi},\mathbf{x},t)$, is a deterministic function of its arguments.

In order to model stochastic properties of turbulent combustion we introduce stochastic fields $\xi_k^*=\xi_k^*(\mathbf{x},t)$. The function $P_\xi=P_\xi(\boldsymbol{\xi};\mathbf{x},t)$, which represents the one-point, one-time joint PDF of $\xi_1^*,\ldots,\xi_{n_r}^*$, is required to satisfy the equation

$$\frac{\partial \langle\rho\rangle P_\xi}{\partial t} + \boldsymbol{\nabla}\cdot(\mathbf{U}\langle\rho\rangle P_\xi) + \frac{\partial A_k\langle\rho\rangle P_\xi}{\partial \xi_k} + \frac{\partial^2 B_{kl}\langle\rho\rangle P_\xi}{\partial \xi_k \partial \xi_l} = 0. \tag{12}$$

This equation is called the reference PDF equation while P_ξ is referred to as the reference PDF. Satisfying the reference PDF equation is a mathematical requirement whose necessity is demonstrated in the following subsection. The values ξ_i^* may be generated/modeled in different ways as long as its PDF complies with (12), although Eq. (12) does not necessarily reflect the physical nature of the fluctuations simulated by ξ_i^*. Depending on the implementation of the model, different ξ_i^* may simulate fluctuations induced by different factors (i.e., by fluctuations of the mixture fraction, fluctuations of velocity, fluctuations of dissipation, etc.). The conservative formulation of the MMC model,

$$\frac{\partial \langle\rho\rangle P_\xi Z_I}{\partial t} + \boldsymbol{\nabla}\cdot(\mathbf{U}\langle\rho\rangle P_\xi Z_I) + \frac{\partial A_k\langle\rho\rangle P_\xi Z_I}{\partial \xi_k} - \langle\rho\rangle P_\xi \Omega_I$$
$$= \frac{\partial}{\partial \xi_k}\left(B_{kl}\langle\rho\rangle P_\xi\frac{\partial Z_I}{\partial \xi_l} - Z_I\frac{\partial B_{kl}\langle\rho\rangle P_\xi}{\partial \xi_l}\right)$$
$$= \frac{\partial}{\partial \xi_k}\left(2B_{kl}\langle\rho\rangle P_\xi\frac{\partial Z_I}{\partial \xi_l} - \frac{\partial B_{kl}\langle\rho\rangle P_\xi Z_I}{\partial \xi_l}\right), \tag{13}$$

can be obtained from Eqs. (11) and (12). This form appears to be convenient for numerical implementations.

Here, we also consider the stochastic fields $Z_I^*=Z_I[\boldsymbol{\xi}^*(\mathbf{x},t),\mathbf{x},t]$, which are represented by deterministic functions of stochastic arguments. The joint PDF of the values $\mathbf{Z}_{\{I\}}^*$ is denoted by $P_Z=P_Z(\mathbf{z}_{\{I\}};\mathbf{x},t)$, where $\mathbf{z}_{\{I\}}$ represent the sample space variables for $\mathbf{Z}_{\{I\}}^*$. The span index I may

vary in the definition of P_Z so that the definition corresponds to the PDFs of different levels. The asterisk superscript is used to indicate the stochastic nature of the variables or fields.

The one-point joint PDF of the n_s fields $\mathbf{Z}^*$ is denoted by $P_Z(\mathbf{z};\mathbf{x},t)$ and, through the relation $\mathbf{Z}^* = \mathbf{Z}[\boldsymbol{\xi}^*(\mathbf{x},t),\mathbf{x},t]$, it can be obtained from P_ξ by

$$P_Z(\mathbf{z};\mathbf{x},t) = \int P_\xi(\boldsymbol{\xi};\mathbf{x},t)\,\delta[\mathbf{Z}(\boldsymbol{\xi},\mathbf{x},t) - \mathbf{z}]d\boldsymbol{\xi},$$

where integration is over the entire reference space. This PDF is the model for the Favre PDF of the species $\widetilde{P}_Y(\mathbf{y};\mathbf{x},t)$. In the following sections the connection between P_Z and $\widetilde{P}_Y$ is established by showing that under certain conditions specified below, the MMC model gives solutions of Eqs. (8) and (9).

This interpretation, of course, assumes a certain link between the coefficients of Eqs. (8) and (9) and (12) and (11) (i.e., MMC has also to be a model for the unknown coefficients N_{IJ} and $\mathbf{u}$). In the following section, it is shown that, generally, the relationships between the coefficients are

$$W_I(\mathbf{z}_{\{J\}};\mathbf{x},t) = \langle \Omega_I^* | \mathbf{Z}_{\{J\}}^* = \mathbf{z}_{\{J\}} \rangle,$$

$$\mathbf{u}(\mathbf{z}_{\{I\}};\mathbf{x},t) = \langle \mathbf{U}^* | \mathbf{Z}_{\{I\}}^* = \mathbf{z}_{\{I\}} \rangle, \tag{14}$$

$$N_{IJ}(\mathbf{z}_{\{K\}};\mathbf{x},t) = \langle N_{IJ}^* | \mathbf{Z}_{\{K\}}^* = \mathbf{z}_{\{K\}} \rangle,$$

where

$$\Omega_I^* \equiv \Omega_I(\mathbf{Z}^*),$$

$$\mathbf{U}^* \equiv \mathbf{U}[\boldsymbol{\xi}^*(\mathbf{x},t),\mathbf{x},t], \quad N_{IJ}^* \equiv N_{IJ}^\circ[\boldsymbol{\xi}^*(\mathbf{x},t),\mathbf{x},t], \tag{15}$$

$$N_{IJ}^\circ(\boldsymbol{\xi},\mathbf{x},t) \equiv B_{kl}\frac{\partial Z_I}{\partial \xi_k}\frac{\partial Z_J}{\partial \xi_l}.$$

The reaction source terms are also included to emphasize that W_I is considered to be a model for W_I in (4). If the set of $Z_I = Z_I(\boldsymbol{\xi},\mathbf{x},t)$ uniquely determines the values of $\xi_k = \xi_k(\mathbf{Z}_{\{I\}},\mathbf{x},t)$ that correspond to $Z_{\{I\}}$, then Eqs. (14) can be simplified. Indeed, in this case the condition $\mathbf{Z}_{\{I\}}^* = \mathbf{z}_{\{I\}}$ uniquely determines the values of $\boldsymbol{\xi}^*$ and the values averaged in (14) cannot fluctuate around their conditional means so that we can write

$$\mathbf{u}[\mathbf{Z}_{\{I\}}(\boldsymbol{\xi},\mathbf{x},t);\mathbf{x},t] = \mathbf{U}(\boldsymbol{\xi},\mathbf{x},t),$$

$$N_{IJ}[\mathbf{Z}_{\{K\}}(\boldsymbol{\xi},\mathbf{x},t);\mathbf{x},t] = N_{IJ}^\circ(\boldsymbol{\xi},\mathbf{x},t). \tag{16}$$

It should be noted that, unless $\mathbf{Z}_{\{I\}}$ and $\boldsymbol{\xi}$ have the same dimension while the functions $Z_I = Z_I(\boldsymbol{\xi},\mathbf{x},t)$ provide one-to-one mappings of $\boldsymbol{\xi}$ into $\mathbf{Z}_{\{I\}}$, not all combinations of $\mathbf{Z}_{\{I\}}^*$ are realizable (i.e., having a positive probability).

D. Compliance with the PDF equation

Although Eqs. (11) for Z_I are deterministic, the values $Z_I^* = Z_I(\boldsymbol{\xi}^*,\mathbf{x},t)$ are stochastic due to the randomness of $\boldsymbol{\xi}^*$. Stochastic values Z_I^* can be characterized by a PDF $P_Z(\mathbf{z}_{\{I\}};\mathbf{x},t)$, which, as it is shown below, is a model for $\widetilde{P}_Y(\mathbf{y}_{\{I\}};\mathbf{x},t)$. In this section the values indexed by I, J, K represent any selected subset of the species or a complete set

of all species while the small indices i, j, k run over all reference variables. Although, in this section, we do not make any explicit assumptions about the dimensions involved, it should be noted that, if the dimension of $\mathbf{Z}_{\{I\}}^*$ exceeds the dimension of $\boldsymbol{\xi}^*$, the PDF $P_Z(\mathbf{z}_{\{I\}};\mathbf{x},t)$ must be singular due to a deterministic functional dependence between some of the values $\mathbf{Z}_{\{I\}}^*$. Conventional generalized interpretation is assigned to all equations dealing with singular PDFs. We demonstrate now that P_Z satisfies Eq. (4) governing $\widetilde{P}_Y$, provided the reference PDF P_ξ satisfies Eq. (12) and the coefficients N_{IJ} and $\mathbf{u}$ are modeled by (16). The proof is based on Bayes theorem in the form

$$P_Z(\mathbf{z}_{\{I\}};\mathbf{x},t) = \int P_{Z|\xi}(\mathbf{z}_{\{I\}}|\boldsymbol{\xi};\mathbf{x},t)P_\xi(\boldsymbol{\xi};\mathbf{x},t)d\boldsymbol{\xi}, \tag{17}$$

where $P_{Z|\xi}$ is the PDF of $\mathbf{Z}_{\{I\}}^*$ conditioned on $\boldsymbol{\xi}^* = \boldsymbol{\xi}$. Since the functions $Z_I(\boldsymbol{\xi};\mathbf{x},t)$ are deterministic, this PDF is given by

$$P_{Z|\xi}(\mathbf{z}_{\{I\}}|\boldsymbol{\xi};\mathbf{x},t) = \delta(\mathbf{Z}_{\{I\}}(\boldsymbol{\xi};\mathbf{x},t) - \mathbf{z}_{\{I\}}), \tag{18}$$

where the Dirac delta function applied to vector arguments denotes the product of delta functions applied to the vector components.

The PDF transport equation for $P_{Z|\xi}$ obtained from Eq. (11) is given by

$$\frac{\partial P_{Z|\xi}}{\partial t} + \mathbf{U}\cdot\boldsymbol{\nabla}P_{Z|\xi} + A_k\frac{\partial P_{Z|\xi}}{\partial \xi_k} + \frac{\partial^2 N_{IJ}^\circ P_{Z|\xi}}{\partial z_I \partial z_J} + \frac{\partial \Omega_I P_{Z|\xi}}{\partial z_I}$$

$$= B_{kl}\frac{\partial^2 P_{Z|\xi}}{\partial \xi_k \partial \xi_l}, \tag{19}$$

where N_{IJ}° is defined in (15). This equation can be derived using the following identities and the standard PDF techniques:

$$\frac{\partial P_{Z|\xi}}{\partial t} = -\frac{\partial}{\partial z_I}\left(P_{Z|\xi}\frac{\partial Z_I}{\partial t}\right), \quad \frac{\partial P_{Z|\xi}}{\partial \xi_k} = -\frac{\partial}{\partial z_I}\left(P_{Z|\xi}\frac{\partial Z_I}{\partial \xi_k}\right),$$

$$\boldsymbol{\nabla}P_{Z|\xi} = -\frac{\partial P_{Z|\xi}\boldsymbol{\nabla}Z_I}{\partial z_I},$$

$$\frac{\partial^2 P_{Z|\xi}}{\partial \xi_k \partial \xi_l} = \frac{\partial^2}{\partial z_I \partial z_J}\left(P_{Z|\xi}\frac{\partial Z_I}{\partial \xi_k}\frac{\partial Z_J}{\partial \xi_l}\right) - \frac{\partial}{\partial z_I}\left(P_{Z|\xi}\frac{\partial^2 Z_I}{\partial \xi_k \partial \xi_l}\right).$$

The last identity is used in the derivation after being multiplied by $B_{kl}(\boldsymbol{\xi};\mathbf{x},t)$ and interpreted in accordance with the definition of N_{IJ}° in (15).

The evolution equation for $P_Z(\mathbf{z}_{\{I\}};\mathbf{x},t)$ is obtained from Eq. (17) by multiplying Eq. (19) by $\langle\rho\rangle P_\xi(\boldsymbol{\xi};\mathbf{x},t)$ and integrating over all $\boldsymbol{\xi}$. The terms involving $\partial/\partial \xi_k$ are integrated by parts. During this integration we also take into account that

$$P_{Z|\xi}(\mathbf{z}_{\{I\}}|\boldsymbol{\xi};\mathbf{x},t)P_\xi(\boldsymbol{\xi};\mathbf{x},t) = P_{\xi|Z}(\boldsymbol{\xi}|\mathbf{z}_{\{I\}};\mathbf{x},t)P_Z(\mathbf{z}_{\{I\}};\mathbf{x},t), \tag{20}$$

and replace $P_{Z|\xi}P_\xi$ by $P_Z P_{\xi|Z}$ in the following integrals:

$$\int N_{IJ}^\circ(\boldsymbol{\xi};\mathbf{x},t)P_{Z|\xi}P_\xi d\boldsymbol{\xi} = \langle N_{IJ}^* | \mathbf{Z}_{\{K\}}^* = \mathbf{z}_{\{K\}} \rangle P_Z$$

$$= N_{IJ}(\mathbf{z}_{\{K\}};\mathbf{x},t)P_Z, \tag{21}$$

$$\int \mathbf{U}(\boldsymbol{\xi}_{\{k\}};\mathbf{x},t)P_{Z|\xi}P_{\xi}d\boldsymbol{\xi}=\langle\mathbf{U}^*|\mathbf{Z}^*_{\{I\}}=\mathbf{z}_{\{I\}}\rangle P_Z$$

$$=\mathbf{u}(\mathbf{z}_{\{I\}};\mathbf{x},t)P_Z, \tag{22}$$

$$\int \Omega_J[\mathbf{Z}(\boldsymbol{\xi},\mathbf{x},t)]P_{Z|\xi}P_{\xi}d\boldsymbol{\xi}=\langle\Omega^*_J|\mathbf{Z}^*_{\{I\}}=\mathbf{z}_{\{I\}}\rangle P_Z$$

$$=W_J(\mathbf{z}_{\{I\}};\mathbf{x},t)P_Z. \tag{23}$$

Here, in these integrals, we use the equations and definitions specified in (14). The result is given by

$$\frac{\partial\langle\rho\rangle P_Z}{\partial t}+\boldsymbol{\nabla}\cdot(\mathbf{u}\langle\rho\rangle P_Z)+\frac{\partial W_I\langle\rho\rangle P_Z}{\partial z_I}+\frac{\partial^2 N_{IJ}\langle\rho\rangle P_Z}{\partial z_I\partial z_J}$$

$$=\int\left(\frac{\partial\langle\rho\rangle P_{\xi}}{\partial t}+\boldsymbol{\nabla}\cdot(\mathbf{U}\langle\rho\rangle P_{\xi})+\frac{\partial A_k\langle\rho\rangle P_{\xi}}{\partial\xi_k}\right.$$

$$\left.+\frac{\partial^2 B_{kl}\langle\rho\rangle P_{\xi}}{\partial\xi_k\partial\xi_l}\right)P_{Z|\xi}d\boldsymbol{\xi}. \tag{24}$$

It is easy to see now that Eq. (12) nullifies the right-hand side of Eq. (24) and results in Eq. (4). That is the joint PDF modeled by MMC satisfies the PDF transport equation provided the reference PDF P_{ξ} complies with the reference PDF equation given by (12).

Another question that may be of interest to the reader is whether the compliance of P_{ξ} with the reference PDF equation is a necessarily condition for the MMC model to be in agreement with the PDF transport equation. In general, it is possible to find an example when the expression in the brackets on the right-hand side of (24) is nonzero but the integral in (24) remains zero. However, if $\mathbf{Z}_{\{I\}}=\mathbf{Z}_{\{I\}}(\xi,\mathbf{x},t)$ uniquely determines a single point $\boldsymbol{\xi}$ in the reference space, then Eq. (12) must be satisfied in order to ensure the compliance of P_Z with the PDF transport equation. Indeed, $P_{Z|\xi}$ defined in (18) represents a delta function, so that for a given point in Z space there is only one point in the ξ space that contributes to the integral in (24). Hence, practically, it would be very difficult to suggest a reasonable mapping model with the reference fields $\boldsymbol{\xi}^*$ whose joint PDF does not comply with Eq. (12).

E. Compliance with the CMC equation

The dimension of the reference space n_r is, generally, expected to be smaller than the total number of species n_s. Thus, the fluctuations of $\mathbf{Z}^*$ lie within a manifold of dimension n_r that can be specified by n_r major variables $\mathbf{Z}^*_{\{i\}}$. If the major variables are selected, then the rest of the variables, $\mathbf{Z}^*_{\{\alpha\}}$, cannot fluctuate independently and can be fully characterized by their conditional expectations $Q_{\alpha}=Q_{\alpha}(\mathbf{z}_{\{i\}};\mathbf{x},t)\equiv\langle Z^*_{\alpha}|\mathbf{Z}^*_{\{i\}}=\mathbf{z}_{\{i\}}\rangle$. As is discussed above, $Q_{\alpha}(\mathbf{y}_{\{i\}};\mathbf{x},t)$ is expected to satisfy the CMC equation (9) for any choice of the major variables that can fully specify the allowed fluctuations. This property of the MMC model is demonstrated below. The conditional transformations considered in this section are not much different from those used by the standard CMC techniques,[8] although they are applied to the "surrogate" modeling variables $\mathbf{Z}^*$ instead of the physical mass fractions $\mathbf{Y}$.

First, we consider a joint PDF $P_Z(\mathbf{z}_{\{I\}};\mathbf{x},t)$ for the set of n_r+1 variables $\mathbf{z}_{\{I\}}=\{\mathbf{z}_{\{i\}},z_{\alpha}\}$. As it is shown in the previous section, the MMC PDF P_Z satisfies Eq. (4). After multiplying this equation by z_{α} and integrating over all z_{α}, we obtain

$$\frac{\partial Q_{\alpha}\langle\rho\rangle P_Z}{\partial t}+\boldsymbol{\nabla}\cdot(\langle\mathbf{U}^*Z^*_{\alpha}|\mathbf{z}_{\{i\}}\rangle\langle\rho\rangle P_Z)+\frac{\partial\langle\Omega^*_i Z^*_{\alpha}|\mathbf{z}_{\{i\}}\rangle\langle\rho\rangle P_Z}{\partial z_i}$$

$$+\frac{\partial}{\partial z_i}\left(\frac{\partial\langle N^*_{ij}Z^*_{\alpha}|\mathbf{z}_{\{i\}}\rangle\langle\rho\rangle P_Z}{\partial z_j}-2\langle N^*_{i\alpha}|\mathbf{z}_{\{i\}}\rangle\langle\rho\rangle P_Z\right)$$

$$=\langle\Omega^*_{\alpha}Z^*_{\alpha}|\mathbf{z}_{\{i\}}\rangle\langle\rho\rangle P_Z. \tag{25}$$

In this section, we use the abbreviation $\langle\cdot|\mathbf{z}_{\{i\}}\rangle$ to denote the conditional expectation $\langle\cdot|\mathbf{Z}^*_{\{i\}}=\mathbf{z}_{\{i\}}\rangle$. Since $\mathbf{Z}_{\{i\}}$ forms a set of major species and the condition $\mathbf{Z}^*_{\{i\}}=\mathbf{z}_{\{i\}}$ is sufficient to specify all fluctuations present in the model, all correlations in (25) can be decoupled. For example, we can write $\langle N^*_{ij}Z^*_{\alpha}|\mathbf{z}_{\{i\}}\rangle=N_{ij}Q_{\alpha}$, and, with the use of Eqs. (15) and (16), $\langle N_{i\alpha}|\mathbf{z}_{\{i\}}\rangle=N_{ij}\partial Q_{\alpha}/\partial z_j$, where $N_{ij}=N_{ij}(\mathbf{z}_{\{i\}};\mathbf{x},t)$ and $Q_{\alpha}=Q_{\alpha}(\mathbf{z}_{\{i\}};\mathbf{x},t)$. After decoupling, Eq. (25) can be easily transformed into the CMC equation given by (9). Thus, the MMC model is compliant with the CMC equations for any proper choice of the conditioning major $\mathbf{Z}^*_{\{i\}}$ and conditioned minor $\mathbf{Z}^*_{\{\alpha\}}$ species.

F. The Gaussian shape of the reference PDF

The MMC equations presented above do not represent yet a complete model. Indeed, the coefficients A_k, B_{kl}, and $\mathbf{U}$ have to be specified consistently with the PDF P_{ξ}. Although other assumptions stipulating the shape of the reference PDF P_{ξ} are possible, in the present work, we follow the ideas of mapping closure[13,14] and require that the values ξ^*_k are stochastically independent while having Gaussian distributions with zero mean and unit dispersion for any $\mathbf{x}$ and t:

$$P_{\xi}(\boldsymbol{\xi})=G(\xi_1)G(\xi_2)\cdots G(\xi_{n_r}),$$

$$G(\xi_k)\equiv\frac{1}{\sqrt{2\pi}}\exp\left(-\frac{\xi^2_k}{2}\right). \tag{26}$$

This PDF satisfies Eq. (12) provided that

$$\mathbf{U}(\boldsymbol{\xi}_{\{k\}};\mathbf{x},t)=\mathbf{U}^{(0)}(\mathbf{x},t)+\mathbf{U}^{(1)}_k(\mathbf{x},t)\xi_k,$$

$$A_k=-\frac{\partial B_{kl}}{\partial\xi_l}+B_{kl}\xi_l+a_k,\quad a_k(\mathbf{x},t)\equiv\frac{1}{\langle\rho\rangle}\boldsymbol{\nabla}\cdot(\langle\rho\rangle\mathbf{U}^{(1)}_k). \tag{27}$$

That is, $\mathbf{U}$ depends linearly on ξ_k. (The linear dependence of conditional velocity on conditioning scalars is repeatedly used in publications.[8,29]) This point can be easily proved by substituting the values of $\mathbf{U}$, B_{kl}, A_k, and P_{ξ} into Eq. (12) and noting the following relations:

$$P_{\xi}\xi_l+\frac{\partial P_{\xi}}{\partial\xi_l}=0,\quad\mathbf{U}^{(0)}=\tilde{\mathbf{v}},\quad\frac{\partial P_{\xi}}{\partial t}=0,\quad\boldsymbol{\nabla}P_{\xi}=0,$$

and

$$\frac{\partial\langle\rho\rangle}{\partial t}+\boldsymbol{\nabla}\cdot(\langle\rho\rangle\mathbf{U})=\xi_k\boldsymbol{\nabla}\cdot(\langle\rho\rangle\mathbf{U}^{(1)}_k).$$

The last relation takes into account the mean continuity equation. Note that $\mathbf{U}^{(0)}=\langle\mathbf{U}\rangle=\tilde{\mathbf{v}}$ since $\langle\xi_k^*\rangle=0$. In MC, it is conventional to assume that B_{kl} is independent of $\boldsymbol{\xi}$:

$$B_{kl}=B_{kl}(\mathbf{x},t). \tag{28}$$

The values of the coefficients $\mathbf{U}^{(0)}$, $\mathbf{U}_k^{(1)}$, and B_{kl} are linked to the well-explored properties of turbulent transport—the Favre mean velocity $\tilde{\mathbf{v}}$, the Favre turbulent fluxes $\widetilde{v''Y_i''}$ and the Favre-averaged dissipation tensor $\tilde{\chi}_{ij}$ of the major species—by the following equations:

$$\mathbf{U}^{(0)}=\tilde{\mathbf{v}}, \quad \mathbf{U}_k^{(1)}\langle\xi_k^* Z_i^*\rangle=\widetilde{v''Y_i''}, \quad B_{kl}\left\langle\frac{\partial Z_i}{\partial\xi_k}\frac{\partial Z_j}{\partial\xi_l}\right\rangle=\tilde{\chi}_{ij}. \tag{29}$$

The Favre averages (whose example is given by $\tilde{\chi}_{ij}=\langle\chi_{ij}\rho\rangle/\langle\rho\rangle$) are the averages evaluated with the use of the Favre PDF $\tilde{P}_Y$. The PDFs P_Z and P_ξ are the conventional PDFs of the stochastic variables $\mathbf{Z}_{\{i\}}^*$ and $\boldsymbol{\xi}^*$, and the averages using these PDFs are shown as conventional. However, one should remember that the conventional PDF P_Z represents a model for the Favre PDF $\tilde{P}_Y$ [i.e., $\tilde{P}_Y(\mathbf{z}_{\{i\}};\mathbf{x},t)=P_Z(\mathbf{z}_{\{i\}};\mathbf{x},t)$]. If the dissipation properties of all scalars are similar (i.e., the same dissipation scale is assumed for all scalars and the differential diffusion effects are neglected) then the approximation,

$$B_{kl}=B(\mathbf{x},t)\delta_{kl}, \tag{30}$$

should be appropriate.

G. Initial conditions

In this section, we consider how the initial mapping of the major species into the reference space can be set in order to comply with a given PDF specified by $\tilde{P}_Y(\mathbf{y}_{\{i\}})=\tilde{P}_Y(\mathbf{y}_{\{i\}},\mathbf{x},t_0)$. The arguments t and $\mathbf{x}$ are, generally, omitted in this section since all considerations are applied to the initial moment $t=t_0$ and a certain point $\mathbf{x}$ in the physical space or its vicinity that is sufficiently small to be treated as spatially homogeneous. The PDFs of minor species are restricted by Eq. (7) and are not considered here.

One of the methods, which allows algorithmically for the setting of the initial conditions $Y_i=Z_i(\boldsymbol{\xi}^*)$, corresponding to the given initial joint PDF, is to follow Pope[14] and use the ordering procedure. The major presumption of this procedure is that $\mathbf{Y}_{\{n_r\}}$ represents an ordered set of the scalars $\{Y_1,Y_2,\ldots,Y_{n_r}\}$ and $\tilde{P}_Y(\mathbf{y}_{\{n_r\}})$ is its joint PDF. (Although some procedures that may serve as a certain justification of the ordering are presented later in the present work when the discrete version of MMC is introduced, ordering of variables in not consistent with the independence principle.[14]) The stochastic reference variables are represented by the ordered set $\boldsymbol{\xi}_{\{n_r\}}^*=\{\xi_1^*,\xi_2^*,\ldots,\xi_{n_r}^*\}$ and their PDF usually assumed Gaussian. The joint PDF determines the series of reduced PDFs $\tilde{P}_Y(y_1),\tilde{P}_Y(y_1,y_2),\ldots,\tilde{P}_Y(\mathbf{y}_{\{n_r\}})$ that can be equivalently represented by the series of the conditional PDFs,

$$\tilde{P}_Y(y_1),$$
$$\tilde{P}_Y(y_2|y_1)=\tilde{P}_Y(y_1,y_2)/\tilde{P}_Y(y_1),$$
$$\ldots,$$
$$\tilde{P}_Y(y_{n_r}|\mathbf{y}_{\{n_r-1\}})=\tilde{P}_Y(\mathbf{y}_{\{n_r\}})/\tilde{P}_Y(\mathbf{y}_{\{n_r-1\}}).$$

At each of n_r steps of the mapping procedure, the mapping is sought to comply with the corresponding reduced PDF. Specifically, at any step I, the mapping $Y_I=Z_I(\xi_I^*,\boldsymbol{\xi}_{\{I-1\}}^*)$ is determined as the monotonic function of ξ_I^*, which matches the conditional PDF $\tilde{P}_Y(y_I|\mathbf{y}_{\{I-1\}})$. The values $\boldsymbol{\xi}_{\{I-1\}}^*$ are treated as parameters of the mapping and $\mathbf{y}_{\{I-1\}}=\mathbf{Z}_{\{I-1\}}(\boldsymbol{\xi}_{\{I-1\}}^*)$ are determined by previous $I-1$ steps. At the first step, the mapping $Y_1=Z_1(\xi_1^*)$ is identical to the one-variable mapping problem while for the other steps mapping is different from one-variable mapping only by the presence of additional parameters. The overall mapping of $\mathbf{Y}_{\{n_r\}}$ into $\boldsymbol{\xi}_{\{n_r\}}^*$ is given by

$$\mathbf{Y}_1=\mathbf{Z}_1(\boldsymbol{\xi}_1^*),$$
$$\mathbf{Y}_2=\mathbf{Z}_2(\boldsymbol{\xi}_1^*,\boldsymbol{\xi}_2^*),\ldots, \quad \mathbf{Y}_{n_r}=\mathbf{Z}_{n_r}(\boldsymbol{\xi}_1^*,\ldots,\boldsymbol{\xi}_{n_r}^*).$$

Although this mapping represents a solution of the initial conditions problem, there are still several questions to be answered. If the variables $\xi_1,\ldots,\xi_{n_r}$ are assumed to be stochastically identical, their ordering does not impose any limitations. The physical scalars $Y_1,\ldots,Y_{n_r}$ are not identical and their ordering can be performed in $n_r!$ different ways.[14] This shows that, generally, the initial mapping is not uniquely determined by the initial joint PDF. The monotonic character of the mapping functions is another restriction, which is, generally, not required by MMC. Without this restriction even one-variable mapping is not unique. We can note that for such complicated phenomenon as turbulence the physical evolution of the PDFs is likely to be determined not only by the initial conditions imposed on the PDFs but also by other parameters of turbulence.[27] The influence of the other parameters is neglected by the models that presume that the initial value of the PDF uniquely determines its evolution. Potentially, the additional freedom in initial mapping can be used to match the effect of the other parameters on evolution of the PDF.

H. Qualitative properties

In the end of this section, we note some quite obvious features of the MMC model, which make its use very attractive. Note that these properties are related to general MMC, while setting the initial conditions by ordering the scalars is not complying with some of the properties. The diffusion/convection part of the MMC model [i.e., we formally put $\Omega_I=0$ in (11)] has the following properties that match well the properties of turbulent transport in a realistic flow.

(i)   The description of the turbulent diffusion and convection by the MMC model is local.
(ii)   The MMC model predictions for scalars and their linear combinations (which satisfy the modeling transport equations) remain bounded.

(iii)   All scalars are treated by the MMC model in the same way without any discrimination.

(iv)   The MMC prediction for the turbulent transport of one scalar is not affected by the other scalars.

(v)   In homogeneous turbulence, the PDFs approximated by the MMC model evolve toward Gaussian PDFs.

Although the localness of the MMC model is related to the localness of the differential operators used in MMC, a more physical consideration of this property is offered in the following sections, where a discrete numerical version of the MMC model is analyzed. The boundedness is a common property of parabolic equations (1) of not exceeding the upper and lower limits specified by the initial maximal and minimal values of Y_I. This property is preserved by Eqs. (11), specifying the MMC model. The relaxation to a Gaussian shape is an obvious common property of MCs using Gaussian reference fields. Although the PDFs of scalars in turbulent flows may be quite different from Gaussian, the PDFs, generally, tend to evolve toward the Gaussian shape unless they are disturbed by boundary conditions or other factors.

III. STOCHASTIC REPRESENTATION OF THE MMC MODEL

The modeling equations specified by (11) can be solved deterministically by a finite difference numerical method. However, obtaining deterministic solution seems problematic for the multidimensional spaces of reference variables $n_r \gg 1$. In this case, using stochastic differential equations utilizing n_r independent Wiener processes $\mathbf{w}^* = \{w_1^*, \ldots, w_{n_r}^*\}$ can be more economical for numerical calculations. The stochastic model is represented by the following system of stochastic Ito equations:

$$d\mathbf{x}^{*p} = \mathbf{U}(\boldsymbol{\xi}^{*p}, \mathbf{x}^{*p}, t)dt, \tag{31}$$

$$d\xi_k^{*p} = A_k^\circ(\boldsymbol{\xi}^{*p}, \mathbf{x}^{*p}, t)dt + b_{kl}(\boldsymbol{\xi}^{*p}, \mathbf{x}^{*p}, t)dw_l^*, \tag{32}$$

$$dZ_I^{*p} = (\bar{W}_I^{*p} + S_I^{*p})dt, \tag{33}$$

$$\bar{W}_I^{*p} \equiv \Omega_I(\bar{\mathbf{Z}}^{*p}), \quad \langle S_I^{*p} | \boldsymbol{\xi}^{*p} = \boldsymbol{\xi}, \mathbf{x}^{*p} = \mathbf{x} \rangle = 0, \tag{34}$$

$$\bar{Z}_I^{*p} \equiv \bar{Z}_I(\boldsymbol{\xi}^{*p}, \mathbf{x}^{*p}, t),$$
$$\bar{Z}_I(\boldsymbol{\xi}, \mathbf{x}, t) \equiv \langle Z_I^{*p} | \boldsymbol{\xi}^{*p} = \boldsymbol{\xi}, \mathbf{x}^{*p} = \mathbf{x} \rangle, \tag{35}$$

$$A_k^\circ \equiv A_k + \frac{2}{P_\xi} \frac{\partial B_{kl} P_\xi}{\partial \xi_l}, \quad 2B_{kl} = b_{ki} b_{li}. \tag{36}$$

We use the superscript ''$*p$'' to distinguish the values linked to stochastic trajectories, which are also called ''stochastic particles.'' Unless the contrary is specified, the capital subscript indices I, J, and K run over all species $1, 2, \ldots, n_s$, while the small indices run over the dimensions of the reference space. The vectors without indices correspond to the vectors of maximal possible dimension for the quantity specified by the vector. The PDF P_ξ of the reference fields is assumed to be known and the values ξ_k^{*p} are used to simulate the diffusion in the reference space (rather than to determine

P_ξ). The goal of the model is to find $\bar{Z}_I(\boldsymbol{\xi}, \mathbf{x}, t)$, which, as it is shown below, satisfies the MMC equations (11).

The value S_I^{*p} is any arbitrary operator that does not alter the conditional expectations, as specified by the second equation in (34). This operator is related to the numerical realization of the model and is discussed later (its purpose is, generally, to keep Z_I^{*p} close to $\bar{Z}_I^{*p}$). At this moment, we only note that the following simple examples of S_I^{*p}—(1) $S_I^{*p} = 0$, and (2) $S_I^{*p} = (\bar{Z}_I^{*p} - Z_I^{*p})/\tau_S$ (where τ_S is a certain relaxation time)—satisfy the required condition in (34).

The system specified by (31)–(36) is equivalent to the following direct Kolmogorov (Fokker–Planck) equation:

$$\frac{\partial P_{FP}}{\partial t} + \boldsymbol{\nabla} \cdot (\mathbf{U} P_{FP}) + \frac{\partial A_k^\circ P_{FP}}{\partial \xi_k} - \frac{\partial^2 B_{kl} P_{FP}}{\partial \xi_k \partial \xi_l} + \frac{\partial (\bar{W}_I + S_I) P_{FP}}{\partial z_I}$$
$$= 0, \tag{37}$$

for the joint PDF,

$$P_{FP} = P_{FP}(\mathbf{z}, \boldsymbol{\xi}, \mathbf{x}; t)$$
$$= \langle \delta[\mathbf{z} - \mathbf{Z}^{*p}(t)] \delta[\boldsymbol{\xi} - \boldsymbol{\xi}^{*p}(t)] \delta[\mathbf{x} - \mathbf{x}^{*p}(t)] \rangle,$$

where $\bar{W}_I \equiv \Omega_I(\bar{\mathbf{Z}})$.

The value $\bar{Z}_I$ defined in (35) can be equivalently represented by

$$\bar{Z}_I(\boldsymbol{\xi}, \mathbf{x}, t) = \frac{F_I(\boldsymbol{\xi}, \mathbf{x}, t)}{F_0(\boldsymbol{\xi}, \mathbf{x}, t)},$$

where the following integrals:

$$F_0(\boldsymbol{\xi}, \mathbf{x}, t) = \int P_{FP} d\mathbf{z}, \quad F_I(\boldsymbol{\xi}, \mathbf{x}, t) = \int P_{FP} z_I d\mathbf{z}, \tag{38}$$

are introduced. The condition in (34) leads to the following constraint:

$$\int P_{FP} S_I d\mathbf{z} = 0, \tag{39}$$

for the operator S_I. In addition to these integrals, we also introduce the quantity m representing the integral of $\langle \rho \rangle$ over the whole physical domain under consideration,

$$m = \int \langle \rho \rangle d\mathbf{x}. \tag{40}$$

The stochastic model introduced in this section represents a stochastic version of the MMC model (although this does not mean, of course, that the model is intended to simulate all stochastic properties of turbulent diffusion). Indeed, assuming that the distribution of the MMC particles [i.e., stochastic trajectories whose evolution is specified by the equations (31)–(38)] is set initially and on boundaries in $\mathbf{x}$ space such that $F_0 = \langle \rho \rangle P_\xi / m$ and $F_I = \langle \rho \rangle Z_I P_\xi / m$, the further evolution of the functions $F_0(\boldsymbol{\xi}, \mathbf{x}, t)$, $F_I(\boldsymbol{\xi}, \mathbf{x}, t)$ and $\bar{Z}_I(\boldsymbol{\xi}, \mathbf{x}, t)$, which are interpreted as

$$F_0 = \frac{\langle \rho \rangle P_\xi}{m}, \quad F_I = \frac{Z_I \langle \rho \rangle P_\xi}{m}, \quad \bar{Z}_I \equiv \frac{F_I}{F_0} = Z_I, \tag{41}$$

satisfy Eqs. (12), (13), and (11) correspondingly. In order to prove this statement we, first, note that the functions F_0 and P_ξ have a consistent normalization,

$$m \int F_0(\boldsymbol{\xi},\mathbf{x},t)d\boldsymbol{\xi}d\mathbf{x} = m = \int \langle\rho\rangle P_\xi(\boldsymbol{\xi};\mathbf{x},t)d\boldsymbol{\xi}d\mathbf{x}.$$

The integrals whose limits are not specified explicitly indicate integrating over all meaningful values of the corresponding variables. The integration of Eq. (37) over all values $\mathbf{z}$ results in disappearing of the last term on the left-hand side of (37). It is easy to see that, since the coefficients A_k°, B_{kl}, and $\mathbf{U}$ do not depend on $\mathbf{z}$, the resultant equation,

$$\frac{\partial F_0}{\partial t} + \boldsymbol{\nabla}\cdot(\mathbf{U}F_0) + \frac{\partial A_k^\circ F_0}{\partial \xi_k} - \frac{\partial^2 B_{kl}F_0}{\partial \xi_k \partial \xi_l} = 0, \qquad (42)$$

can be converted into (12) by substituting $F_0 = \langle\rho\rangle P_\xi/m$ and the definition of A_k° in (36) into Eq. (42). Thus, if initially $F_0 = \langle\rho\rangle P_\xi/m$, this link between F_0 and P_ξ is preserved during the evolution of the stochastic model.

The integration of (37) over all values $\mathbf{z}$ can also be performed after multiplying (37) by z_I. In this case, the last term on the left-hand side of Eq. (37) does not disappear and it has to be integrated by parts to yield

$$\frac{\partial F_I}{\partial t} + \boldsymbol{\nabla}\cdot(\mathbf{U}F_I) + \frac{\partial A_k^\circ F_I}{\partial \xi_k} - \frac{\partial^2 B_{kl}F_I}{\partial \xi_k \partial \xi_l} = \bar{W}_I F_0. \qquad (43)$$

The term involving S_I disappears due to the constraint specified by Eq. (39). With the use of A_k° defined by (36) this equation can be transformed into

$$\frac{\partial F_I}{\partial t} + \boldsymbol{\nabla}\cdot(\mathbf{U}F_I) + \frac{\partial A_k F_I}{\partial \xi_k}$$
$$+ \frac{\partial}{\partial \xi_k}\left(\bar{Z}_I \frac{\partial B_{kl}F_0}{\partial \xi_l} - B_{kl}F_0 \frac{\partial \bar{Z}_I}{\partial \xi_l}\right) = \bar{W}_I F_0, \qquad (44)$$

provided $F_0 = \langle\rho\rangle P_\xi/m$. Equation (44) is equivalent to (13) since $\bar{W}_I = \Omega_I(\bar{\mathbf{Z}})$. Equations (44) and (42) determine that

$$\frac{\partial \bar{Z}_I}{\partial t} + \mathbf{U}\cdot\boldsymbol{\nabla}\bar{Z}_I + A_k \frac{\partial \bar{Z}_I}{\partial \xi_k} - B_{kl}\frac{\partial^2 \bar{Z}_I}{\partial \xi_k \partial \xi_l} = \bar{W}_I. \qquad (45)$$

Equation (45) coincides with Eq. (11).

The stochastic version of the MMC model allows for a different interpretation. Let us introduce a conditional probability $P_{Z|\xi}(\mathbf{z},\boldsymbol{\xi},\mathbf{x},t)$ so that $P_{FP} = P_{Z|\xi}F_0$. Equations (36), (37), and (42) determine that $P_{Z|\xi}$ satisfies the equation

$$\frac{\partial P_{Z|\xi}}{\partial t} + \mathbf{U}\cdot\boldsymbol{\nabla}P_{Z|\xi} + A_k\frac{\partial P_{Z|\xi}}{\partial \xi_k} + \frac{\partial(W_I + S_I)P_{Z|\xi}}{\partial z_I}$$
$$= B_{kl}\frac{\partial^2 P_{Z|\xi}}{\partial \xi_k \partial \xi_l}, \qquad (46)$$

which appears to be consistent with (19), provided

$$S_I P_{Z|\xi} = \frac{\partial N_{IJ}^\circ P_{Z|\xi}}{\partial z_J}. \qquad (47)$$

Here and in (36) we replace $\bar{W}_I$ by $W_I = \Omega_I(Z)$. This equation provides a new definition of $N_{IJ}^\circ = N_{IJ}^\circ(\mathbf{z},\boldsymbol{\xi},\mathbf{x},t)$ that de-

pends on $\mathbf{z}$ and complies with restriction (39). Since $P_{Z|\xi}$ satisfies (19) and $F_0 = \langle\rho\rangle P_\xi/m$ satisfies (12), then as it is shown in Sec. II D, the PDF P_Z, defined by

$$P_Z(\mathbf{z}_{\{I\}};\mathbf{x},t) = \frac{m}{\langle\rho\rangle}\int P_{FP}d\boldsymbol{\xi} = \frac{m}{\langle\rho\rangle}\int P_{Z|\xi}F_0 d\boldsymbol{\xi} \qquad (48)$$

—the equivalent of Eq. (17)—satisfies Eq. (4). Thus, the distribution of the stochastic particles in the Z-x space represents a consistent model for the joint scalar PDF $\tilde{P}_Y$. According to this interpretation of the MMC model, the minor fluctuations are not neglected, although their modeling is not as detailed as modeling of major fluctuations. The dissipation of minor fluctuations is specified by operator S_I. The characteristic dissipation time τ_S [that is used in a simple relaxation model $S_I = (\bar{Z}_I - Z_I)/\tau_S$] should be selected to match the physical dissipation properties if the minor fluctuations are not neglected. The dissipation N_{IJ} that represents the average of N_{IJ}° over $\boldsymbol{\xi}$ as specified in (21) is a model for the scalar dissipation tensor. It should be noted that this value may fluctuate around N_{IJ} introduced on the basis of Eqs. (15) and (21).

IV. NUMERICAL IMPLEMENTATION

The MMC model can be implemented by solving a finite-difference representation of the deterministic equations given by (11) and, for low dimensions $n_r \sim 1$, this would be an efficient and simple method. The situation is changed for multidimensional problems $n_r \gg 1$. Indeed, the evaluation of diffusion terms on a regular grid requires consideration of at least three node points in each direction totaling to 3^{n_r} points in the finite-difference neighborhood of each node. Such evaluations are computationally problematic. For multidimensional spaces, an efficient numerical implementation requires using the Monte-Carlo (stochastic particles) methods.[4] In these methods, the PDFs are represented by n_p discrete particles. With the use of the delta functions we can replace P_{FP} by

$$P_{FP}^*(\mathbf{Z},\boldsymbol{\xi},\mathbf{x};t) = \frac{1}{n_p}\sum_{p=1}^{n_p}\delta[\mathbf{Z}-\mathbf{Z}^{*p}(t)]\delta[\boldsymbol{\xi}-\boldsymbol{\xi}^{*p}(t)]\delta[\mathbf{x}$$
$$-\mathbf{x}^{*p}(t)], \qquad (49)$$

where the evolution of $\mathbf{Z}^{*p}(t)$, $\boldsymbol{\xi}^{*p}(t)$, and $\mathbf{x}^{*p}(t)$ is governed by (31)–(36). Hence, the function F_0 and F_I are replaced by

$$F_0^*(\boldsymbol{\xi},\mathbf{x};t) = \frac{1}{n_p}\sum_{p=1}^{n_p}\delta[\boldsymbol{\xi}-\boldsymbol{\xi}^{*p}(t)]\delta[\mathbf{x}-\mathbf{x}^{*p}(t)], \qquad (50)$$

$$F_I^*(\boldsymbol{\xi},\mathbf{x};t) = \frac{1}{n_p}\sum_{p=1}^{n_p}\bar{Z}_I^{*p}(t)\delta[\boldsymbol{\xi}-\boldsymbol{\xi}^{*p}(t)]\delta[\mathbf{x}-\mathbf{x}^{*p}(t)]. \qquad (51)$$

One should be able to evaluate the conditional expectations $\bar{Z}_I^{*p}$ while using the discrete representations of P_{FP},

$$\bar{Z}_I^{*p}(t) = \frac{\sum_{q=1}^{n_p}g^{pq}Z_I^{*q}(t)}{\sum_{q=1}^{n_p}g^{pq}}. \qquad (52)$$

The non-negative weights g^{pq} specify the contribution of particle q to the conditional average evaluated at the location of particle p in the $\mathbf{x}$-$\boldsymbol{\xi}$ space. The shape of this function is to be determined later. At the moment, we only note that g^{pq} should rapidly tend to zero as the distance between the particles in the $\mathbf{x}$-$\boldsymbol{\xi}$ space increases. Effectively, this means that the sums are to be evaluated, not over all n_p particles, but only over n_p' particles ($n_p' < n_p$), located in the vicinity of the particle p. Equation (52) can be rewritten as

$$\bar{Z}_I^{*p}(t) = \sum_{q=1}^{n_p} \hat{g}^{pq} Z_I^{*q}(t), \quad \hat{g}^{pq} = \frac{g^{pq}}{\sum_{r=1}^{n_p} g^{pr}}. \tag{53}$$

The interaction matrix $\hat{g}^{pq}$ defined in (53) satisfies the normalization condition

$$\sum_{q=1}^{n_p} \hat{g}^{pq} = 1. \tag{54}$$

We assume that the coefficients of the model are specified as in (27) and the initial distribution of the particles in $\mathbf{x}$-$\boldsymbol{\xi}$ space is set according to $F_0 = \langle \rho \rangle P_\xi / m$ with Gaussian P_ξ given by (26). (Note that this distribution is preserved during integration.) For each time step Δt, the increments of the particles' properties are decomposed into three substeps: transport (drift), mixing (diffusion), and reaction. This subdivision is neither unique nor compulsory for the method—the purpose of the subdivision is, mainly, to simplify the presentation and analysis by focusing on certain features at a time. Unless the contrary is specified, the substeps are applied consecutively: the initial conditions for the following substep are set by the final conditions for the previous substep. The procedure of numerical integration is now analyzed for each of these substeps.

A. The transport (drift) substep

For this substep we evaluate only the drift-type terms (with the exception of the reaction terms that are evaluated separately). The equations for this step can be formally obtained by putting $B_{kl} = 0$, $b_{kl} = 0$, $S_I = 0$, and $W_I^\circ = 0$:

$$d\mathbf{x}^{*p} = \mathbf{U} dt, \quad d\xi_k^{*p} = A_k^\circ dt, \quad dZ_I^{*p} = 0. \tag{55}$$

These equations are integrated by a finite-difference method between t_1 and $t_2 = t_1 + \Delta t$. Note that, for this substep, $d\bar{Z}_I^{*p} = 0$ since Eqs. (42) and (43) take the form

$$\frac{\partial F_{I^\circ}}{\partial t} + \nabla \cdot (\mathbf{U} F_{I^\circ}) + \frac{\partial A_k^\circ F_{I^\circ}}{\partial \xi_k} = 0, \quad I^\circ = 0,1,\ldots,n_s. \tag{56}$$

This equation determines that, for the transport substep,

$$\frac{\partial \bar{Z}_I}{\partial t} + \mathbf{U} \cdot \nabla \bar{Z}_I + A_k^\circ \frac{\partial \bar{Z}_I}{\partial \xi_k} = 0, \tag{57}$$

and $\bar{Z}_I$ is preserved along the characteristics of Eq. (57) specified by (55).

B. The mixing (diffusion) substep

For this substep we put $A_k^\circ = 0$, $\mathbf{U} = 0$, and $W_I = 0$ to evaluate the evolution due to diffusion in $\boldsymbol{\xi}$ space by

$$d\mathbf{x}^{*p} = \mathbf{0}, \quad d\xi_k^{*p} = b_{kl} dw_l, \quad dZ_I^{*p} = S_I^{*p} dt. \tag{58}$$

The operator S_I^{*p} is related to the mixing substep since its purpose is to keep Z_I^{*p} close to $\bar{Z}_I^{*p}$. The finite difference representation of this equation that is to be integrated between t_1 and $t_2 = t_1 + \Delta t$, is given by

$$\Delta \xi_k^{*p} = b_{kl} \bar{w}_l^* \sqrt{\Delta t}, \tag{59}$$

where b_{kl} is assumed to be constant during this time step and $\bar{w}_l^*$ represents independent Gaussian stochastic values with zero mean and unit variance. In the rest of this section we assume that $S_I^{*p} = 0$ and $dZ_I^{*p} = 0$. Note that, for this substep $\bar{Z}_I$ is not preserved (even if $S_I^{*p} = 0$) and has to be reevaluated, as specified by Eq. (52). Indeed, Eqs. (42) and (43) now take the form

$$\frac{\partial F_{I^\circ}}{\partial t} = \frac{\partial^2 B_{kl} F_{I^\circ}}{\partial \xi_k \partial \xi_l}, \quad I^\circ = 0,1,\ldots,n_s, \tag{60}$$

which, generally, does not allow for $\partial \bar{Z}_I / \partial t = 0$ (where $\bar{Z}_I = F_I / F_0$). Let us assume that $Z_I^{*p} = \bar{Z}_I^{*p}$ before the time step. After the diffusion substep Z_I^{*p} remains unchanged (assuming $S_I^{*p} = 0$) but $\bar{Z}_I^{*p}$ changes so that the values Z_I^{*p} would have a growing dispersion around their conditional means specified by $\bar{Z}_I^{*p}$.

C. The reaction substep

For this substep we put $S_I = 0$, $B_{kl} = 0$, $b_{kl} = 0$, $A_k^\circ = 0$, and $\mathbf{U} = 0$ so that

$$d\mathbf{x}^{*p} = \mathbf{0}, \quad d\xi_k^{*p} = 0, \quad dZ_I^{*p} = W_I(\bar{\mathbf{Z}}^{*p}) dt. \tag{61}$$

As it is determined by Eqs. (50), (51), and (52), the conditional expectations satisfy the following equation:

$$\frac{\partial \bar{Z}_I}{\partial t} = W_I(\bar{\mathbf{Z}}) \Rightarrow d\bar{Z}_I^{*p} = W_I(\bar{\mathbf{Z}}^{*p}) dt. \tag{62}$$

Hence, $d\bar{Z}_I^{*p} = dZ_I^{*p}$. Since, for this substep, the particles do not move in $\boldsymbol{\xi}$-$\mathbf{x}$ space, the partial time derivatives are no different from an ordinary time derivative. Equation (62) is to be integrated between t_1 and $t_2 = t_1 + \Delta t$, and this determines the increments of both $d\bar{Z}_I^{*p}$ and dZ_I^{*p}. Considering that the reaction rates usually represent a system of stiff differential equations, Eq. (62) is more preferable than (61). Because of the stiffness, the reaction substep is always placed last, and the most prudent way of evaluating the reaction substep is to solve the reaction equations in conjunction with mixing,

$$\frac{d\bar{Z}_I^{*p}}{dt} = W_I(\bar{\mathbf{Z}}^{*p}) + \left(\frac{d\bar{Z}_I^{*p}}{dt} \right)_{\text{mix}}, \tag{63}$$

where the last term represents the rate of change due to the mixing process, which is obtained from the mixing substep. Equation (63) is to be integrated between t_1 and $t_2 = t_1 + \Delta t$ from initial conditions set before the mixing substep.

Phys. Fluids, Vol. 15, No. 7, July 2003

Model for turbulent reactive flows   1917

D. The mixing substep using diffusing clouds

The major features of the transport, mixing, and reaction substeps are discussed in the previous sections. An evaluation of the transport substep is not difficult and can be achieved by standard techniques. Although an evaluation of the reaction substep is not easy due to stiffness of the chemical kinetics, these problems are well investigated and not specifically discussed in the present work. Our focus in this section is on the implementation of the mixing substep that can be done in different ways corresponding to different values of the exchange matrix $\hat{g}^{pq}$.

When Y_I is modeled by $\bar{Z}_I^*$, the analysis of the previous section indicates that the values Z_I^{*p} are needed only to evaluate the conditional expectations $\bar{Z}_I^{*p}$. If the values $\bar{Z}_I^{*p}$, which represent conditional expectations of Z_I^{*p} assigned to the particles, can be evaluated directly during the diffusion substep then Z_I^{*p} are not needed. Avoiding using Z_I^{*p} promises some other benefits. If the calculations are based on Z_I^{*p}, then their dispersion around $\bar{Z}_I^{*p}$ will grow with time. This would make the accurate evaluation of $\bar{Z}_I^{*p}$ by (52) more difficult and would require a larger number of particles for averaging. In the present section we demonstrate that the direct evaluation of $\bar{Z}_I^{*p}$ from the transport equations during the diffusion substep effectively determines the best value for g^{pq}. The influence of mixing can be assessed in a semistochastic manner: each discrete particle is replaced by a diffusing cloud that expands with time. At the end of each mixing substep, the particle positions are to be regenerated in accordance with density of superimposed clouds.

The coefficient B_{kl}, as it is defined in (28), does not depend on $\boldsymbol{\xi}$ (otherwise, we can assume that B_{kl} remains constant in a vicinity of a certain point of the ξ space). Assuming that B_{kl} remains constant during the time step Δt and that the flow is homogeneous in physical space (or can be treated as such for a selected cell in physical space), let us determine the evolution of $\mathbf{F}_{\{I^\circ\}} = \{F_0, \mathbf{F}_{\{I\}}\}$ during the diffusion substep from the initial conditions specified at $t = t_1$. The substep is controlled by Eq. (60). This evolution is represented by the integral

$$F_{I^\circ}(\boldsymbol{\xi}, t_2) = \int F_{I^\circ}(\boldsymbol{\xi}^\circ, t_1) g_f(\boldsymbol{\xi} - \boldsymbol{\xi}^\circ, \Delta t) d\boldsymbol{\xi}^\circ, \qquad (64)$$

where $t_2 = t_1 + \Delta t$, and the function $g_f = g_f(\Delta\boldsymbol{\xi}, \Delta t)$ represents the fundamental solution of (60), which is defined by the initial condition

$$g_f(\Delta\boldsymbol{\xi}, 0) = \delta(\Delta\boldsymbol{\xi}),$$

and specified by

$$g_f(\Delta\boldsymbol{\xi}, \Delta t) = \frac{1}{(B 4\pi\Delta t)^{n_r/2}} \exp\left(\frac{B_{kl}^{-1}\Delta\xi_k\Delta\xi_l}{4\Delta t}\right),$$
$$B = \det(B_{ij})^{1/n_r}. \qquad (65)$$

Note the replacement of $\boldsymbol{\xi}$ by $\boldsymbol{\xi}'$ so that $\xi_k = b_{il}\xi_l'$ converts B_{kl} in Eq. (60) into a unit matrix.

Considering the discrete representation of F_{I° in (50) and (51) for $t = t_1$, we should replace the integral in (64) by the Monte Carlo sum

$$F_{I^\circ}(\boldsymbol{\xi}, t_2) = \frac{1}{n_p} \sum_{p=1}^{n_p} \bar{Z}_{I^\circ}^{*p}(t_1) g_f(\boldsymbol{\xi} - \boldsymbol{\xi}^{*p}(t_1), \Delta t), \qquad (66)$$

where n_p represents the number of particles in the selected physical cell and we formally put $\bar{Z}_0 \equiv 1$. Equations (66) determine that

$$\bar{Z}_{I^\circ}(\boldsymbol{\xi}, t_2) = \frac{F_I}{F_0} = \frac{\sum_{p=1}^{n_p} \bar{Z}_I^{*p}(t_1) g_f[\boldsymbol{\xi} - \boldsymbol{\xi}^{*p}(t_1), \Delta t]}{\sum_{p=1}^{n_p} g_f[\boldsymbol{\xi} - \boldsymbol{\xi}^{*p}(t_1), \Delta t]}. \qquad (67)$$

After the time step, the distribution of the particles in $\boldsymbol{\xi}$ space is no longer represented by Eq. (50), so that we have to redistribute the particles according to the continuous F_0 specified by (66). Of course, we cannot increase the number of particles to reflect that $F_0(t_2)$ is smooth and the number of particles is to be kept the same for all time steps. The most simple way of redistributing particles is to alter the position of each particle in $\boldsymbol{\xi}$ space by $\Delta\xi_k^{*p} = b_{kl}\bar{w}_l^*\sqrt{\Delta t}$ as it is specified in (59) with the same Δt as in Eq. (66). One can see that the PDF of the Gaussian increments $\Delta\xi_k^{*p}$ coincides with g_f specified by (65). The new values of $\bar{Z}_I^{*q}(t_2) = \bar{Z}_I[\boldsymbol{\xi}^{*q}(t_2), t_2]$ are given by the equation

$$\bar{Z}_I^{*q}(t_2) = \frac{\sum_{p=1}^{n_p} \bar{Z}_I^{*p}(t_1) g_f[\boldsymbol{\xi}^{*q}(t_2) - \boldsymbol{\xi}^{*p}(t_1), \Delta t]}{\sum_{p=1}^{n_p} g_f[\boldsymbol{\xi}^{*q}(t_2) - \boldsymbol{\xi}^{*p}(t_1), \Delta t]}, \qquad (68)$$

obtained from (67). Equations (66) and (68) correspond to Eq. (53),

$$\bar{Z}_I^{*p}(t_2) = \sum_{q=1}^{n_p} \hat{g}^{pq} \bar{Z}_I^{*q}(t_1), \qquad (69)$$

with the following interaction matrix $\hat{g}^{qp}$:

$$\hat{g}^{pq} = \frac{g^{pq}}{g^p}, \quad g^p = \sum_{r=1}^{n_p} g^{pr},$$
$$g^{pq} = g_f[\boldsymbol{\xi}^{*p}(t_2) - \boldsymbol{\xi}^{*q}(t_1), \Delta t]. \qquad (70)$$

Note that the averaging effect is achieved here by advancing the distributions in time from t_1 to $t_2 = t_1 + \Delta t$. The rate of mixing that corresponds to (70) is determined by the finite difference representation,

$$\left(\frac{d\bar{Z}_I^{*p}}{dt}\right)_{\text{mix}} = \frac{\bar{Z}_I[\boldsymbol{\xi}^{*p}(t_2), t_2] - \bar{Z}_I^{*p}(t_1)}{\Delta t}$$
$$= \frac{\sum_{q=1}^{n_p} \hat{g}^{pq} \bar{Z}_I^{*q}(t_1) - \bar{Z}_I^{*p}(t_1)}{\Delta t}. \qquad (71)$$

Practically the sums are evaluated only over $n_p' < n_p$ particles that make a significant contribution to (68). The volume in $\boldsymbol{\xi}$ space, where g_f is essentially positive can be assessed as $V_\xi = (B 4\pi\Delta t)^{n_r/2}$. (Considering that the integral of the fundamental solution remains unity, we use the inverse of the maximal value of the function g_f as the volume estimation.) Here, we use the isotropic value B for estimations. The number of particles used for averaging is then assessed as $n_p' \sim V_\xi / d_1^{n_r}$, where d_1 is the average distance between particles in $\boldsymbol{\xi}$ space while $\bar{d}_1^{n_r}$ represents an estimation of the

ξ-space volume per particle. The relative stochastic error in the evaluation of the convolution integral is estimated as $E_{fs} \sim (n_p')^{-1/2}$. Hence, the number of particles n_p' should be sufficiently large to keep the stochastic error small, and this requirement constrains the minimum time step Δt. (The minimum time gets smaller when larger ensembles of particles are used in calculations.) At the same time, very large values of Δt [although giving precise values of $F_{I^\circ}^{*p}(t_2)$ at $t_2 = t_1 + \Delta t$] would not be accurate in the evaluation of the time derivative by $[F_{I^\circ}^{*p}(t_2) - F_{I^\circ}^{*p}(t_1)]/\Delta t$. The relative error in the representation of $F_{I^\circ}^{*p}(t_2)$ by the first-order scheme can be estimated $E_{ft} \sim (\Delta t/\Delta t_f)^2$, where $\Delta t_f \sim d_f^2/B$ is the time scale of the problem and d_f is the characteristic ξ scale of the problem. Hence, $E_{fs} \sim [d_1^2/(B\Delta t)]^{n_r/4} \sim (d_1/d_f)^{n_r/2}(\Delta t_f/\Delta t)^{n_r/4}$. By equating the order of the errors $E_{ft} \sim E_{fs}$, we obtain $E_{ft} \sim (d_1/d_f)^{n_r/2} E_{ft}^{-n_r/8}$. The relative error in representation of the time derivative is given by $E_{dt} \sim (\Delta t/\Delta t_f) \sim E_{ft}^{1/2}$. These considerations result in

$$E_{dt} \sim \left(\frac{d_1}{d_f} \right)^{2/(8/n_r + 1)}.$$

For very large dimensions $n_r \gg 1$, the relative error in the representation of the time derivative is proportional to $(d_1/d_f)^2$, where d_f/d_1 represents the spatial resolution. Hence, the considered scheme is, asymptotically at $n_r \rightarrow \infty$, second-order accurate in space.

Since $n_p' \sim E_{fs}^{-2} \sim E_{dt}^{-4}$ and $d_1 \sim n_p^{-1/n_r}$, we can write $n_p' \sim (d_f/d_1)^{8/(8/n_r + 1)} \sim (n_p/n_f)^{8/(n_r + 8)}$, where $n_f \equiv d_f^{-n_r}$ is the number of particles that corresponds to the scale d_f. Thus, the rate of increase of n_p' is much slower than that of n_p when n_r is large:

$$n_p' \sim n_p^{8/(n_r + 8)}.$$

The mixing time step Δt can be estimated from $n_p' \sim (B\Delta t/d_1^2)^{n_r/2}$ so that

$$\Delta t \sim \frac{1}{B} \left(\frac{n_p'}{n_p} \right)^{2/n_r} \sim \frac{d_1^2}{B} \left(\frac{d_f}{d_1} \right)^{16/(8 + n_r)}.$$

Note that $\Delta t \rightarrow 0$ as $d_1 \rightarrow 0$ for any $n_r \geq 1$.

The number of operations required for the evaluation of the mixing substep can be assessed as $n_r n_p n_p'$. In order to achieve good performance, the exponent in the fundamental solution $g_f(\cdots)$ should be replaced by a similar but computationally faster function. As expected, the diffusing clouds method becomes more numerically efficient and accurate for large dimensions n_r. Evaluation of averages according to Eq. (52) unavoidably involves a numerical diffusion in ξ space since it has to be conducted over a certain volume. In the diffusing clouds method this numerical diffusion coincides with the rate of diffusion in ξ space required by the MMC model. Compared to this method, any overaveraging would result in excessive numerical diffusion while any underaveraging would cause an excessive stochastic error in the evaluation of $\bar{Z}_I^{*p}$.

The diffusing clouds method (or other similar methods) allows for a different interpretation of its equations. Although, in this section, we attempted to evaluate $\bar{Z}_I^{*p}$ directly

without using Z_I^{*p}, the values we found still involve a stochastic error. These values fluctuating around conditional averages $\bar{Z}^{*p}$ can be also interpreted as Z_I^{*p} with $Z_I^{*p} \rightarrow \bar{Z}_I^{*p}$ as $n_p \rightarrow \infty$. The operator S, which is used in (58) and corresponds to the diffusing clouds method with a mixing rate specified by (71), is given by

$$S_I^{*p} = \frac{1}{\Delta t} \left(\sum_{q=1}^{n_p} \hat{g}^{pq} Z_I^{*q} - Z_I^{*p} \right). \tag{72}$$

This equation can be interpreted as

$$S_I^{*p} = \frac{\bar{Z}_I^{*p} - Z_I^{*p}}{\Delta t}, \quad \bar{Z}_I^{*p} = \sum_{q=1}^{n_p} \hat{g}^{pq} Z_I^{*q}, \tag{73}$$

with Δt representing the relaxation time.

E. Localness of MMC models

The diffusing clouds method is not the only method that can be used for an evaluation of the mixing substep. Any form of the operator S_I that preserves the conditional expectations and reduces fluctuations around the conditional means may potentially be suitable. New versions of the diffusing clouds method can be obtained by using different specifications of $\hat{g}^{pq}$ that are used in (69) or in (72), depending on an interpretation of the model. The major requirements for the interaction matrix $\hat{g}^{pq}$ are the following: (1) localness: $\hat{g}^{pq} \rightarrow 0$ when particles p and q are away from each other; (2) preserving well-mixed conditions $\Sigma_q \hat{g}^{pq} = 1$ [as specified by (54)]; and (3) conservativeness of the scheme $\Sigma_p \hat{g}^{pq} = 1$. Requirements (1) and (2) are satisfied by diffusing clouds exactly while requirement (3) is satisfied by a presented version of the diffusing clouds only approximately.

Another relatively simple possibility is given by the MMC version of the Curl's[30] model: each pair of particles p and q that are closest to each other in ξ space have their values of $\mathbf{Z}^{*p}$ and $\mathbf{Z}^{*q}$ reset to their average $(\mathbf{Z}^{*p} + \mathbf{Z}^{*q})/2$. The particles continue their random motion in ξ space and, after a certain period of time, form new pairs. Whenever two particles get close to each other in ξ space and a new pair is formed, the averaging process is repeated. Curl's model corresponds to the interaction matrix with $\hat{g}^{pq} = \hat{g}^{pp} = \hat{g}^{qp} = \hat{g}^{qq} = 1/2$ for interacting particles and $\hat{g}^{pq} = 0$ for noninteracting couples. In spite of its simplicity, the MMC-Curl model satisfies all three requirements for $\hat{g}^{pq}$.

Although Curl's model is simpler compared to the diffusing clouds method, the diffusing clouds model has the advantage of combining averaging with the effect of diffusion in the reference space, while averaging is effectively achieved by using the fundamental solution (65) of the diffusion equation. The fundamental solution advances the distributions in time, and new values of $\bar{\mathbf{Z}}_I^*$ are calculated from old values, as specified by Eq. (68). In the case of other methods of evaluating the mixing substep, the diffusion is simulated by random particle motions in ξ space and further averaging, which, generally, must be localized in ξ space. In fact, due to the discrete numerical representation of the distributions, averaging can only be performed over a certain ξ

Phys. Fluids, Vol. 15, No. 7, July 2003

Model for turbulent reactive flows   1919

vicinity of each particle. The characteristic size of this vicinity is determined by the average distance between particles. Thus, unless the number of particles is infinite, averaging over a finite vicinity would create an additional numerical diffusion in ξ space.

MMC, in its generalized interpretation, is not restricted to a particular mixing scheme. The major difference between the MMC model and conventional mixing models is related to the following features of MMC: (1) particle positions in the reference ξ space are traced; and (2) only the particles that are close to each other in ξ space (and in the physical $\mathbf{x}$ space) are allowed to be mixed. The second condition provides the localness of the MMC mixing operators. Some of the reference variables can be used to simulate diffusion of the fluid particles in the velocity phase space (note that $\mathbf{U}$ is a linear function of $\boldsymbol{\xi}$ and ξ conditioning effectively represents velocity conditioning) but the meaning of reference variables in mapping closures should not be reduced to simulating only velocity-type conditioning. The reference variables represent a sampling scalar behavior in a turbulent field that can be used to simulate the scalar PDFs. The events that are physically close to each other should have the values of the reference variables that are also close to each other. This condition ensures the localness of the MMC model, which is further refined with an increasing number of the reference variables.

The EMST mixing model[23] performs mixing locally in the species space ($\mathbf{z}$ space). But by using distances measured in $\mathbf{z}$ space, the EMST mixing model violates the linearity and independence principles of scalar mixing.[24] In contrast, MMC performs mixing locally in $\boldsymbol{\xi}$ space, and thereby satisfies these linearity and independence principles.

F. Setting the initial conditions

In this section we use some ideas of Sec. II G and consider how the initial conditions can be set for the particles. We assume that the initial conditions for all species are represented by the distribution of n_p particles,

$$Z_I^{*p}(t_0)=Z_I^{op}, \quad I=1,\ldots,n_s, \quad p=1,\ldots,n_p.$$

Here, as in the previous considerations, we either consider a homogeneous case or apply our consideration to a physical cell, which is sufficiently small so that spatial variations within the cell can be neglected. If the initial distribution in Z-space is specified by the PDF, the particles should first be distributed in accordance with this PDF. The MMC model requires the specification, not only of Z_I^{op}, but also that of the reference variables values $\xi_k^{*p}(t_0)=\xi_k^{op}$ ($k=1,\ldots,n_r$) so that the distribution of the particles in the reference n_r-dimensional space is Gaussian. In the case of multidimensional spaces, this procedure of mapping the values Z_I^{op} into the Gaussian reference space is not unique. The choice of a particular mapping should be based on physical considerations. In the rest of this section we suggest an algorithmic mapping procedure, which, in our opinion, corresponds to the physical nature of the problem.

It is assumed here that the scaling of the values Z_I corresponds to the actual physical significance of each variable

(otherwise Z_I can always be rescaled). First, we form the following correlation matrix:

$$K'_{IJ}=\frac{1}{n_p}\sum_{p=1}^{n_p} Z_I'^p Z_J'^p, \quad Z_I'^p=Z_I^{op}-\frac{1}{n_p}\sum_{p=1}^{n_p} Z_I^{op}.$$

This matrix is, obviously, symmetric $K'_{IJ}=K'_{JI}$ and positive semidefinite. Hence, with the use of the singular value decomposition (svd), we can achieve that

$$K''_{IJ}=K_{(I)}\delta_{IJ}=\frac{1}{n_p}\sum_{p=1}^{n_p} Z_I''^p Z_J''^p=M_{IK}K_{KL}M_{JL},$$

$$Z_I''^p=M_{IK}Z_K'^p,$$

where no sum is taken over the bracketed index I in the second term of the first equation, the matrix M_{IJ} is unitary and K_I are the singular values. The mapping is to be performed using $Z_i''^p$ (i.e., the first n_r values of $Z_I''^p$ that correspond to the n_r largest singular values K_i). The values $Z_i''^p$ represent a good choice for the major subspace.

The particles are then sorted according to the values $Z_1''^p$ so that, for new indices $q=q(p)$, we have $Z_1''^1 \leqslant \cdots \leqslant Z_1''^q \leqslant \cdots \leqslant Z_1''^{n_p}$. For $k=1$, the values ξ_k^{oq} are assigned according to the equation

$$\xi_k^{oq}=\Phi^{-1}\left(\frac{q-1/2}{n_p}\right), \tag{74}$$

where Φ^{-1} represents the inverse of the standardized Gaussian cumulative distribution function,

$$\Phi(\xi')=\int_{-\infty}^{\xi'} G(\xi)d\xi.$$

The particles are sorted into several groups with close values of ξ_1^{oq} (each group represents particles that are effectively conditioned on a given value of ξ_1^{oq}). This algorithm ensures that the particle distribution in the space of the variable ξ_1^{oq} is Gaussian with zero mean and unit dispersion.

The procedure, which is specified in the previous paragraph, is then repeated separately for the particles of each group: the particles are sorted within each group according to their values $Z_2''^p$ and the new indices q are calculated. The values ξ_k^{oq} are calculated according to (74) for $k=2$, new values of q and n_p specifying the number of particles in each of the groups. Thus, the distribution of particles in the ξ_2^{oq} space conditioned on a given value of ξ_1^{oq} is also Gaussian with zero mean and unit dispersion. Each of the groups is then split into subgroups with close values of ξ_2^{oq}. The procedure is then repeated for the rest of the variables $\xi_3^{oq},\ldots,\xi_{n_r}^{oq}$. At each level k of the procedure, the particles are conditioned on the values of $\xi_1^{oq},\ldots,\xi_{k-1}^{oq}$ and their conditional distribution in the space of ξ_k^{oq} is set to be Gaussian with zero mean and unit dispersion (i.e., it is independent of the conditioning variables). At each level, each group of particles is redistributed into subgroups unless the number of particles in the groups is too small. In this case the number of particles is not sufficient to evaluate distributions with multiple conditioning and reduction of the dimension of the reference space to k may be reasonable. Alternatively (if the

dimension of the reference space is not to be reduced), the group subdivision process has to be terminated, although the sorting and assigning process continues.

It is easy to see that the joint distribution of particles in the space of $\xi_1^{oq}, \ldots, \xi_{n_r}^{oq}$ is Gaussian, as it is required in the present formulation of the MMC model. Indeed, the PDF $P_\xi(\xi_1;t_0)$ is Gaussian, and all of the conditional PDFs $P_\xi(\xi_k, \ldots, \xi_{n_r}|\xi_1, \ldots, \xi_{k-1};t_0) = G(\xi_k) \ldots G(\xi_{n_r})$ are Gaussian for any $1 < k < n_r$. Hence, the joint PDF $P_\xi(\boldsymbol{\xi})$ is Gaussian. We note that this procedure is based on the presumption that the various directions in Y space are not equivalent (which is true for many practical cases). Effectively, the method ranks species or directions according to their level of fluctuations. This makes the initial conditions for some species dependent on initial conditions for other species. We will call this method as "mapping by preferential directions."

V. THE THREE-STREAM MIXING PROBLEM IN HOMOGENEOUS TURBULENCE

The multidimensional mapping closure used in the MMC method allows for the evaluation of multidimensional PDFs for two and more independent mixture fractions without any need of ordering or preferential treatment of the variables. The case, which is considered in this section, corresponds to mixing of three regions in homogeneous turbulence. This problem requires two independent mixture fractions Y_1 and Y_2. The initial conditions are set at $t=0$ in accordance with JP[26] so that the regions have the same probability and the following:

$$\text{Region 1: } Y_1 = 0, \quad Y_2 = 1,$$

$$\text{Region 2: } Y_1 = -\frac{\sqrt{3}}{2}, \quad Y_2 = -\frac{1}{2}, \tag{75}$$

$$\text{Region 3: } Y_1 = \frac{\sqrt{3}}{2}, \quad Y_2 = -\frac{1}{2}.$$

Although the method of mapping by preferential directions can be used to set the initial conditions for the three-stream mixing problem, the best choice seems to utilize directly the symmetrical nature of the problem. The conditions are set in the three symmetrically equivalent regions:

$$\text{Region 1: } 0 < \varphi < \frac{2}{3}\pi,$$

$$\text{Region 2: } \frac{2}{3}\pi < \varphi < \frac{4}{3}\pi, \tag{76}$$

$$\text{Region 3: } \frac{4}{3}\pi < \varphi < 2\pi,$$

where we introduce the polar coordinates r_ξ and φ in the space of the reference variables,

$$\xi_1 = r_\xi \sin(\varphi), \quad \xi_2 = r_\xi \cos(\varphi).$$

One can see that the sectors assigned to each of the regions are equivalent for the purposes of the MMC model.

A. Comparison of the analytical solution and DNS

The MMC formulation of the three-stream problem given above has an analytical solution that is compared in this section with the DNS of JP. The major steps of the analytical solution are outlined below. The MMC equation is

$$\frac{\partial Z_i}{\partial t} + B(t)\left(\xi_k \frac{\partial Z_i}{\partial \xi_k} - \frac{\partial^2 Z_i}{\partial \xi_k \partial \xi_k}\right) = 0, \tag{77}$$

where $i,k = 1,2$, and we have taken into account that the scalars are conserved ($W_i = 0$). This can be rewritten in the form

$$\frac{\partial Z_i}{\partial T} + r_\xi \frac{\partial Z_i}{\partial r_\xi} - \frac{1}{r_\xi} \frac{\partial}{\partial r_\xi}\left(r_\xi \frac{\partial Z_i}{\partial r_\xi}\right) - \frac{1}{r_\xi^2} \frac{\partial^2 Z_i}{\partial \varphi^2} = 0,$$

where

$$T = \int_0^t B\,dt.$$

With the use of new variables,

$$\tau = \frac{1 - \exp(-2T)}{2}, \quad r = r_\xi \exp(-T),$$

we obtain

$$\frac{\partial Z_i}{\partial \tau} = \frac{1}{r} \frac{\partial}{\partial r}\left(r \frac{\partial Z_i}{\partial r}\right) + \frac{1}{r^2} \frac{\partial^2 Z_i}{\partial \varphi^2}. \tag{78}$$

The solution of this equation is given by

$$Z_1 = -\sqrt{3} F_r\left(\frac{r}{\sqrt{\tau}}, \varphi\right) - \frac{\sqrt{3}}{2} F_r\left(\frac{r}{\sqrt{\tau}}, \varphi + \frac{2\pi}{3}\right),$$

$$Z_2 = \frac{3}{2} F_r\left(\frac{r}{\sqrt{\tau}}, \varphi + \frac{2\pi}{3}\right), \tag{79}$$

where

$$F_r(R, \varphi) = \sum_{\nu=1}^{\infty} F_\nu(R) \Phi_\nu(\varphi), \quad R \equiv \frac{r}{\sqrt{\tau}},$$

$$F_\nu(R) = \frac{\nu}{2^{\nu+1}} \frac{\Gamma\left(\frac{\nu}{2}\right)}{\Gamma(\nu+1)} R^\nu \, {}_1F_1\left(\frac{\nu}{2}, \nu+1, -\frac{R^2}{4}\right),$$

$$\Phi_\nu(\varphi) = 2 \frac{(-1)^\nu}{\pi\nu} \sin\left(\frac{\pi\nu}{3}\right) \cos(\nu\varphi),$$

$\Gamma(\cdots)$ is the gamma function, and ${}_1F_1(\cdots)$ is the confluent hypergeometric function. The details of this solution are given in the Appendix.

The analytical results obtained in this section and shown to provide a good match to the simulated joint PDF of JP.[26] The value $\sigma = \sigma(t)$ denotes the variance of the scalars $\sigma^2 = \langle(Z_1^*)^2\rangle = \langle(Z_2^*)^2\rangle$ (note that $\langle Z_1^*\rangle = \langle Z_2^*\rangle = 0$). The initial conditions specified by (75) correspond to $\sigma_0^2 = 1/2$ and $\sigma_0 \approx 0.707$, where $\sigma_0 = \sigma(0)$. In the DNS of JP, the initial value was $\sigma_0' \approx 0.627$. In Fig. 1, we follow JP and plot the contour plots for the joint PDF for the same values of $\sigma/\sigma_0' (= 0.8, 0.7, 0.6, 0.5, 0.4,$ and $0.2)$ that correspond to σ/σ_0 of 0.71,
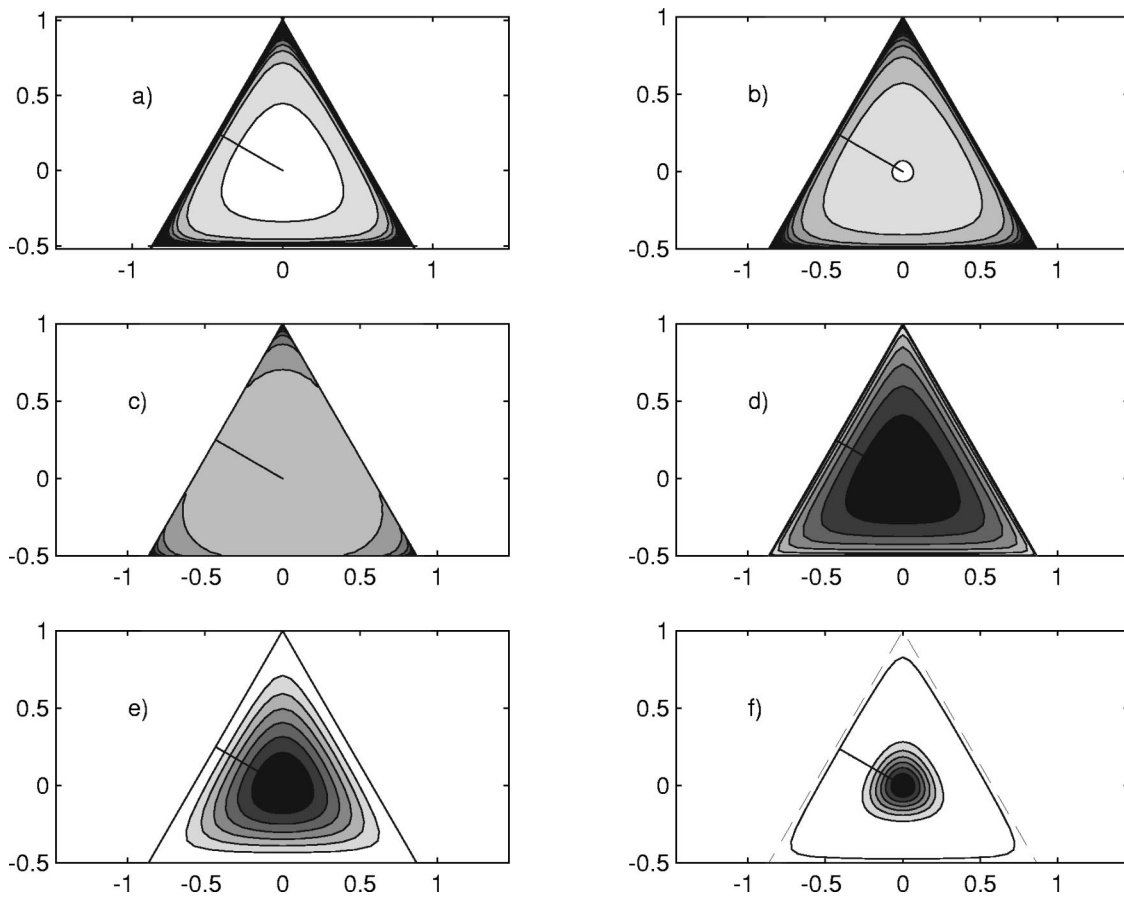
FIG. 1. The consecutive contour plots of the joint PDF for the three-stream mixing problem predicted by the MMC model.

0.62, 0.53, 0.44, 0.35, and 0.18. Figure 2 shows several three-dimensional surface plots for $\sigma/\sigma_0' = 0.55$, 0.5, 0.4, and 0.2 that correspond to $\sigma/\sigma_0 \approx 0.49$, 0.44, 0.35, and 0.18. (The three-dimensional PDF plots for larger values of σ/σ_0 are difficult to visualize.) For $\sigma/\sigma_0 \approx 0.46$, the PDF goes through rapid transformations and becomes almost flat. This corresponds well to the effects observed by JP. Another feature, which can be observed in JP and the present calculations, is that the mixing process is initially more intensive along the sides of the triangle. As is expected, in the final stages of the evolution the PDF is close to Gaussian in both JP and the present calculations. We also note that due to the analytical form of the solution, the three peaks are sharper than in the DNS of JP.

B. Comparison of numerical evaluation and the analytical solution

The problem specified by initial conditions (75) and (76) has also been solved numerically, using the discrete stochastic representation of MMC. The mixing step was evaluated by the diffusing clouds method. The numerical solution should simulate not only the shape of the PDF but also the dissipation rate. Thus, for the result of this section, we specify the time T, which coincides with the physical time t when $B = 1$. The stochastic values ξ_1^* and ξ_2^* have normal distributions with unit dispersions and are not shown here.

The values of Z_1^* and Z_2^* are shown in Fig. 3 by 900

scatter points for the time moments $T = \{0.1, 0.5, 1\}$. Each point represents a "stochastic particle" with 1/900 of the total probability and the density of the points is proportional to the values of joint PDF. The left column of Fig. 3[(a),(c),(e)] represents results $(Z_I^*)_N$ obtained by diffusing clouds. The right column of Fig. 3[(b), (d), (f)] represents the values $(Z_I^*)_A = Z_I[(\boldsymbol{\xi}^*(T), T]$, analytically evaluated at the stochastic locations $\boldsymbol{\xi}^*(T)$ using Eqs. (79). The correlation coefficient defined by $C_Z \equiv \langle (Z_I^*)_A (Z_I^*)_N \rangle / (\sigma_A \sigma_N)$ exceeds 0.99 for all plots in Fig. 3. [Note that $\langle Z_I^* \rangle = 0$ is used in the definition of C_Z; σ_A and σ_N represent the standard deviations of $(Z_I^*)_A$ and $(Z_I^*)_N$ so that $C_Z = 1$ corresponds to the case of perfect agreement $(Z_I^*)_A = (Z_I^*)_N$.] We should also emphasize the stochastic nature of the presented results: the distribution of points exhibits certain fluctuations of density. These fluctuations remain small if a large number of particles is used in the calculations but a larger-than-average fluctuation is always possible. For example, a "bold spot" that can be noticed near the top corner of the triangle in Figs. 3(c) and 3(d) represents a relatively large fluctuation. It is interesting that the spot is well replicated in both Figs. 3(c) and 3(d).

The relative dispersion of the scalars σ/σ_0 is plotted versus time in Fig. 4. The solid line corresponds to the analytical solution, the dashed line shows the expected decay rate for large T, while the symbols correspond to calculations with 900, 90, and 9 particles. Distances between sym-
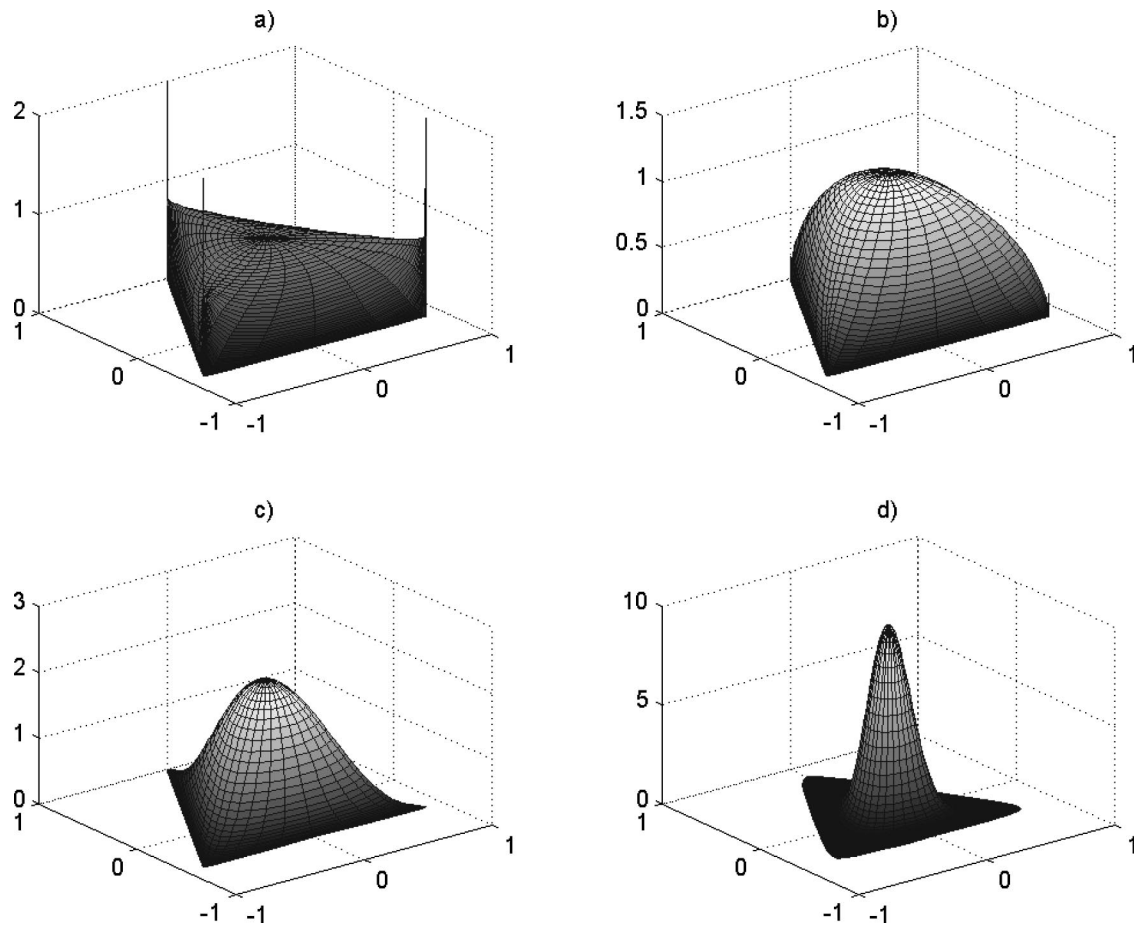
FIG. 2. The consecutive three-dimensional surface plots of the joint PDF for the three-stream mixing problem predicted by the MMC model.
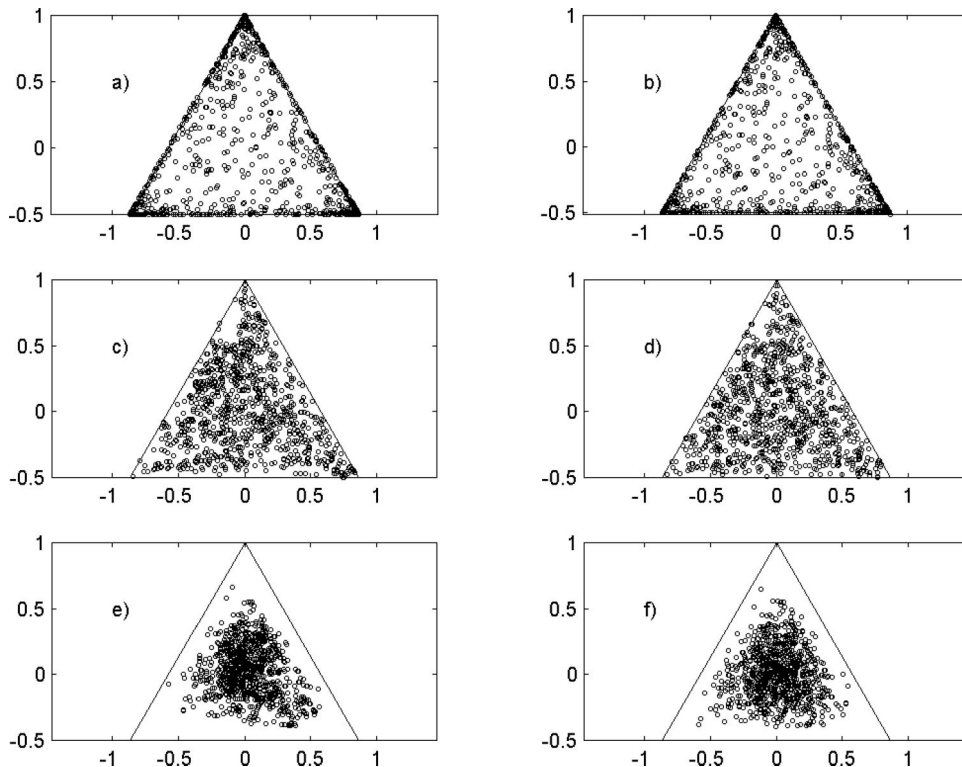

FIG. 3. The scatter plots of the values Z_1^* and Z_2^* calculated numerically using diffusing clouds with 900 particles (left column) and obtained analytically (right column). The results are shown for $T=0.1$ (a), (b); $T=0.5$ (c), (d); and $T=1$ (e), (f).
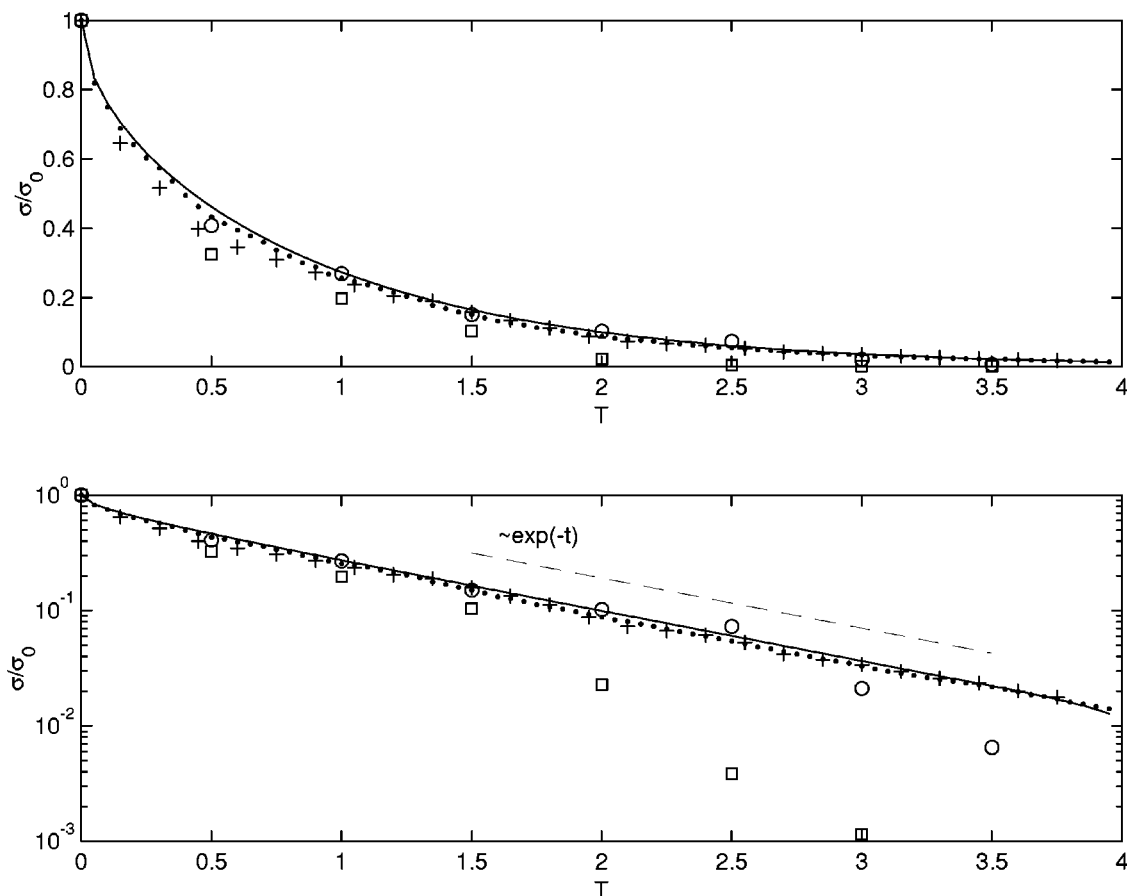
FIG. 4. The relative dispersion σ/σ_0 versus time T: analytical evaluation (—), numerical $n_p = 900$ ($\cdots$), numerical $n_p = 90$ (+++), numerical $n_p = 9$ ($\bigcirc\bigcirc\bigcirc$), and numerical $n_p = 9$ ($\square\square\square$).

bols correspond to the selected time steps. Two cases are shown for $n_p = 9$ to demonstrate stochastic variations of the solution. As can be expected, the precision of the numerical scheme improves with increasing the number of particles n_p.

VI. CONCLUSIONS

In this work we have introduced a new approach to turbulent reactive flows based on multiple mapping conditioning (MMC). In essence, this formulation brings together the CMC and PDF approaches. From the CMC perspective, the present approach represents a generalization to conditioning on n_r variables, with a consistent determination of the joint PDF and conditional dissipation of these variables. From the PDF perspective, the approach embodies the idea that the compositions are confined to an n_r-dimensional manifold in composition space, and it then provides (implicitly) a mixing model, which is the extension of the mapping closure to multiple scalars and inhomogeneous flows. In contrast to previously proposed mixing models,[23,30–34] the present model reflects the physics of mixing in all of the following respects: the mixing is local in composition space;[22,23] the boundedness of scalars[4] is preserved; the model satisfies the linearity and independence principles;[24] and, in appropriate limits, the resulting joint PDF tends to a joint normal distribution. The closure used in the model is validated by a com-

parison with the two-variable joint PDF obtained in DNS by Juneja and Pope[26] for the three-stream mixing problem. The agreement with DNS results is good.

We also give a stochastic equivalent formulation of the MMC model that is expected to be more computationally efficient for multidimensional spaces. The resulting method is similar to a particle implementation of PDF methods, but with the particles having additional properties, namely reference variables ξ_k^{*p}. The treatment of the mixing process is based on the method of diffusing clouds (introduced in the paper) that forces the numerical diffusion to match the diffusion rate required by the model. For the test problem of three-stream mixing, the numerical method of diffusing clouds preforms well compared to the analytical solution of the same problem.

Future directions in the development within the MMC framework include (a) accounting for the intermittency of scalar dissipation, (b) coupling the method with the PDF of velocity for inhomogeneous flows, and (c) application to a variety of turbulent reactive flows.

ACKNOWLEDGMENTS

APPENDIX: ANALYTICAL SOLUTION FOR THE THREE-STREAM MIXING PROBLEM

We consider the equation

$$\frac{\partial f_r}{\partial \tau} = \frac{1}{r}\frac{\partial}{\partial r}\left(r\frac{\partial f_r}{\partial r}\right) + \frac{1}{r^2}\frac{\partial^2 f_r}{\partial \varphi^2}, \tag{A1}$$

for the reference function $f_r = f_r(r, \tau, \varphi)$, and demonstrate that the series

$$f_r(r, \tau, \varphi) = \sum_{\nu=1}^{\infty} f_\nu(r, \tau)\Phi_\nu(\varphi), \tag{A2}$$

where

$$\Phi_\nu(\varphi) = 2\frac{(-1)^\nu}{\pi\nu}\sin\left(\frac{\pi\nu}{3}\right)\cos(\nu\varphi), \tag{A3}$$

$$f_\nu(r, \tau) = \nu\int_0^\infty \exp(-\tau\lambda^2)J_\nu(r\lambda)\frac{d\lambda}{\lambda}, \tag{A4}$$

and J_ν is the Bessel function, represents the solution of Eq. (A1) with the following initial conditions:

$$f_r(r,0,\varphi) = \begin{cases} -1/3, & 0 < \varphi < 2\pi/3 \\ 2/3, & 2\pi/3 < \varphi < 4\pi/3 \\ -1/3, & 2\pi/3 < \varphi < 2\pi \end{cases}. \tag{A5}$$

Indeed, the substitution of (A2) into (A1) results in

$$\frac{\partial f_\nu}{\partial \tau} = \frac{1}{r}\frac{\partial}{\partial r}\left(r\frac{\partial f_\nu}{\partial r}\right) - \frac{\nu^2}{r^2}f_\nu, \tag{A6}$$

while substituting (A4) in (A6), yields the identity

$$\frac{\partial^2 J_\nu}{\partial r^2} + \frac{1}{r}\frac{\partial J_\nu}{\partial r} + \left(\lambda^2 - \frac{\nu^2}{r^2}\right)J_\nu = 0,$$

which defines the Bessel function. Compliance with initial conditions (A5) becomes obvious if we note that[35]

$$f_\nu(r,0) = \nu\int_0^\infty J_\nu(r\lambda)\frac{d\lambda}{\lambda} = 1,$$

for any $r > 0$ and $\nu = 1, 2, 3, \ldots$.

The problem considered here allows for a self-similar formulation. With $f_r(r, \tau, \varphi) = F_r(R, \varphi)$, where $R = r/\tau^{1/2}$, Eq. (A1) takes the form

$$\frac{1}{2}R\frac{\partial F_r}{\partial R} = \frac{1}{R}\frac{\partial}{\partial R}\left(R\frac{\partial F_r}{\partial R}\right) + \frac{1}{R^2}\frac{\partial^2 F_r}{\partial \varphi^2}, \tag{A7}$$

while its solution with the boundary conditions

$$F_r(R, \varphi) \rightarrow \begin{cases} -1/3, & 0 < \varphi < 2\pi/3 \\ 2/3, & 2\pi/3 < \varphi < 4\pi/3 \\ -1/3, & 4\pi/3 < \varphi < 2\pi \end{cases}, \quad \text{as } R \rightarrow \infty,$$

which correspond to the initial conditions (A5) is given by

$$F_r(R, \varphi) = \sum_{\nu=1}^{\infty} F_\nu(R)\Phi_\nu(\varphi), \tag{A8}$$

$$F_\nu(R) = \nu\int_0^\infty \exp(-\lambda^2)J_\nu(R\lambda)\frac{d\lambda}{\lambda} = f_\nu(R\sqrt{\tau}, \tau). \tag{A9}$$

An evaluation of the integral in (A9) [or that in (A4)] indicates that[35]

$$F_\nu(R) = \frac{\nu}{2^{\nu+1}}\frac{\Gamma\left(\frac{\nu}{2}\right)}{\Gamma(\nu+1)}R^\nu {}_1F_1\left(\frac{\nu}{2}, \nu+1, -\frac{R^2}{4}\right)$$

$$= \frac{\nu}{2^{\nu+1}}\frac{\Gamma\left(\frac{\nu}{2}\right)}{\Gamma(\nu+1)}R^\nu {}_1F_1\left(\frac{\nu}{2}+1, \nu+1, \frac{R^2}{4}\right)\exp\left(-\frac{R^2}{4}\right),$$

where $\Gamma(\cdots)$ is the gamma function, ${}_1F_1(\cdots)$ is the confluent hypergeometric function. The last form of the integral is somewhat larger but it is preferable for numerical evaluation of the expression.

The last step in obtaining the analytical solution is to express the values of Z_1 and Z_2 in terms of the function $F_r(R, \varphi)$. It is easy to see that Z_1 and Z_2 defined by (79) satisfy the initial conditions set in (75). [Note that the function F_r with a constant phase shift still satisfies Eq. (A7).]

[1]P. A. Libby and F. A. Williams, *Turbulent Reactive Flows* (Academic, London, 1994).

[2]S. B. Pope, "Computations of turbulent combustion: Progress and challenges," *Twenty-third Symposium (International) on Combustion* (The Combustion Institute, Pittsburgh, 1990), p. 591.

[3]N. Peters, *Turbulent Combustion* (Cambridge University Press, Cambridge, 2000).

[4]S. B. Pope, "Pdf methods for turbulent reactive flows," Prog. Energy Combust. Sci. **11**, 119 (1985).

[5]C. Dopazo, "Recent developments in Pdf methods," in *Turbulent Reacting Flows*, edited by P. A. Libby and F. A. Williams (Academic, London, 1994), Chap. 7, pp. 375–474.

[6]U. A. Maas and S. B. Pope, "Simplifying chemical kinetics: Intrinsic low-dimensional manifolds in composition space," Combust. Flame **88**, 239 (1992).

[7]C. J. Sung, C. K. Law, and J.-Y. Chen, "An augmented reduced mechanism for methane oxidation with comprehensive global parametric validation," *Twenty-seventh Symposium (International) on Combustion* (The Combustion Institute, Pittsburgh, 1998), p. 295.

[8]A. Y. Klimenko and R. W. Bilger, "Conditional moment closure for turbulent combustion," Prog. Energy Combust. Sci. **25**, 595 (1999).

[9]N. Swaminathan and R. W. Bilger, "Conditional variance equation and its analysis," in *Proceedings of the Combustion Institute*, Vol. 27 (The Combustion Institute, Pittsburgh, 1998), pp. 1191–1198.

[10]A. Y. Klimenko, "Conditional methods in application for Lagrangian modelling," Phys. Fluids **10**, 922 (1998).

[11]K. A. Weinman and A. Y. Klimenko, "Estimation of the Kolmogorov constant C_0 by DNS of a continuous scalar," Phys. Fluids **12**, 3205 (2000).

[12]C. M. Cha, G. Kosaly, and H. Pitsch, "Modelling extinction and reignition in turbulent nonpremixed combustion using a doubly-conditioned moment closure approach," Phys. Fluids **13**, 3824 (2001).

[13]H. Chen, S. Chen, and R. H. Kraichnan, "Probability distribution of a stochastically advected scalar field," Phys. Rev. Lett. **63**, 2657 (1989).

[14]S. B. Pope, "Mapping closures for turbulent mixing and reaction," Theor. Comput. Fluid Dyn. **2**, 255 (1991).

[15]F. Gao, "An analytic solution for the scalar probability density function in homogeneous turbulence," Phys. Fluids A **3**, 511 (1991).

[16]S. S. Girimaji, "A mapping closure for turbulent scalar mixing using a time-evolving reference field," Phys. Fluids A **4**, 2875 (1992).

[17] E. E. O'Brien and A. Sahay, "Asymptotic behavior of the amplitude mapping closure," Phys. Fluids A **4**, 1773 (1992).

[18] L. Valiño, J. Ros, and C. Dopazo, "Monte Carlo implementation and analytic solution of an inert-scalar turbulent-mixing test problem using a mapping closure," Phys. Fluids A **3**, 2191 (1991).

[19] L. Valiño and F. Gao, "Monte Carlo implementation of a single-scalar mapping closure for diffusion in the presence of chemical reaction," Phys. Fluids A **4**, 2062 (1992).

[20] F. Gao and E. E. O'Brien, "A mapping closure for multispecies Fickian diffusion," Phys. Fluids A **3**, 956 (1991).

[21] L. Valiño, "Multiscalar mapping closure for mixing in homogeneous turbulence," Phys. Fluids **7**, 144 (1995).

[22] A. T. Norris and S. B. Pope, "Turbulent mixing model based on ordered pairing," Combust. Flame **83**, 27 (1990).

[23] S. Subramaniam and S. B. Pope, "A mixing model for turbulent reactive flows based on Euclidean minimum spanning trees," Combust. Flame **115**, 487 (1998).

[24] S. B. Pope, "Consistent modeling of scalars in turbulent flows," Phys. Fluids **26**, 404 (1983).

[25] J. J. Monaghan, "Smoothed particle hydrodynamics," Annu. Rev. Astron. Astrophys. **30**, 543 (1992).

[26] A. Juneja and S. B. Pope, "A DNS study of turbulent mixing of two passive scalars," Phys. Fluids **8**, 2161 (1996).

[27] S. B. Pope, *Turbulent Flows* (Cambridge University Press, Cambridge, 2000).

[28] A. Y. Klimenko, "Note on conditional moment closure in turbulent shear flows," Phys. Fluids **7**, 446 (1995).

[29] V. R. Kuznetsov and V. A. Sabelnikov, *Turbulence and Combustion* (Hemisphere, New York, 1989).

[30] R. L. Curl, "Dispersed phase mixing. I," AIChE J. **9**, 175 (1963).

[31] J. Villermaux and J. C. Devillon, "Représentation de la coalescence et de la redispersion des domaines de ségrégation dans un fluide par un modèle d'interaction phénoménologique," in *Proceedings of the 2nd International Symposium on Chemical Reaction Engineering* (Elsevier, New York, 1972), pp. 1–13.

[32] C. Dopazo and E. E. O'Brien, "An approach to the autoignition of a turbulent mixture," Acta Astronaut. **1**, 1239 (1974).

[33] J. Janicka, W. Kolbe, and W. Kollmann, "Closure of the transport equation for the probability density function of turbulent scalar fields," J. Non-Equilib. Thermodyn. **4**, 47 (1977).

[34] L. Valiño and C. Dopazo, "A binomial Langevin model for turbulent mixing," Phys. Fluids A **3**, 3034 (1991).

[35] A. P. Prudnikov, Yu. A. Brychkov, and O. I. Marichev, *Integrals and Series* (Gordon and Breach Science, New York, 1986).